Magnetic susceptibility of a CuO$_2$ plane in the La$_2$CuO$_4$ system:
I. RPA treatment of the Dzyaloshinskii-Moriya Interactions

K. V. Tabunshchyk[*]

Department of Physics, Queen's University, Kingston ON K7L 3N6 Canada and
Institute for Condensed Matter Physics, Lviv, Ukraine

R. J. Gooding

Department of Physics, Queen's University, Kingston ON K7L 3N6 Canada
(Dated: February 2, 2008)

Motivated by recent experiments on undoped La$_2$CuO$_4$, which found pronounced temperature-dependent anisotropies in the low-field magnetic susceptibility, we have investigated a two-dimensional square lattice of $S = 1/2$ spins that interact via Heisenberg exchange plus the symmetric and anti-symmetric Dzyaloshinskii-Moriya anisotropies. We describe the transition to a state with long-ranged order, and find the spin-wave excitations, with a mean-field theory, linear spin-wave analysis, and using Tyablikov's RPA decoupling scheme. We find the different components of the susceptibility within all of these approximations, both below and above the Néel temperature, and obtain evidence of strong quantum fluctuations and spin-wave interactions in a broad temperature region near the transition.

I. INTRODUCTION

Quantum magnetism of low-dimensional systems has attracted considerable attention in recent years, in part due to the strong interest in the cuprate superconductors. For example, it has been postulated that a strong antiferromagnetic (AF) exchange interaction may be responsible for the high-temperature superconductivity in these compounds.[1]

The ubiquitous structural and electronic constituent of this latter class of materials is the CuO$_2$ plane, and in this paper we consider the magnetic properties of such planes in their undoped state. In particular, we consider the temperature dependence of the static, uniform magnetic susceptibility for a single plane in an undoped La$_2$CuO$_4$ crystal. This system is known to be an AF insulator with a very simple structure, namely it can be approximately thought of as one CuO$_2$ plane stacked between LaO planes, with this structural unit repeated, in a body-centred tetragonal pattern, throughout all space. However, a small orthorhombic distortion introduces important spin-orbit couplings into the magnetic Hamiltonian, leading to an AF state with a weak canted ferromagnetic moment. These spin-orbit interactions are central to the results presented in this paper.

As was known from the start of research on the cuprate superconductors, a complete knowledge of the properties of the spin-$\frac{1}{2}$ quantum Heisenberg AF on a square lattice is an absolute necessity.[2] However, some experiments have demonstrated that a complete description of the magnetic behaviour found in, *e.g.* La$_2$CuO$_4$, requires additional physics. Examples include (i) weak ferromagnetism in the low-temperature orthorhombic (LTO) phase;[3,4] (ii) spin wave gaps with in- and out-of-plane modes;[5] and perhaps most importantly, (iii) the unusual anisotropy of the magnetic susceptibility observed by Lavrov, Ando, Komiya and Tsukada.[6] It was this latter

experiment that led us to complete a sequence of theoretical investigations on a model that should describe such a three-dimensional array of such CuO$_2$ planes modelling La$_2$CuO$_4$, a structure similar to those found in many cuprate superconductors. This manuscript summarizes the first of these studies, that concerned with a single CuO$_2$ plane, with this plane described by a near-neighbour Heisenberg model plus spin-orbit couplings as embodied by the antisymmetric and symmetric Dzyaloshinskii-Moriya (DM) interactions.[7,8]

An important point needs to be raised to clarify the applicability of this work to a real physical system, such as La$_2$CuO$_4$. Firstly, note that according to the Mermin-Wagner theorem a two-dimensional (2D) system with a continuous symmetry cannot undergo a continuous phase transition, at any nonzero temperature, to a state with true long-ranged order. However, when one includes both the antisymmetric and symmetric DM interactions this symmetry is lifted, and thus the model that we study in this paper will have a true phase transition to an ordered phase at some nonzero temperature, which we shall label by T_N, in analogy to the Néel ordering temperature of a pure antiferromagnet. So, the ordered phase for our model *of a single plane* will include a weak ferromagnetic canted moment, as well as long-ranged AF order. Note that current estimates[9] of another interaction present in the physical La$_2$CuO$_4$ system, that being a very weak AF interlayer coupling which is usually denoted by $J_\perp$, is that this energy scale is close to that of the DM interactions, and thus it is likely that both this exchange and the DM interactions are roughly equally responsible for the observed transition. This serves to emphasize that our study of a single plane is not expected to accurately explain *all* of the observed magnetic properties of La$_2$CuO$_4$; in fact, this work stands alone as a theoretical study of an isolated plane, but it is of considerable interest to learn which experimental data can and which data can not be explained by such a single-plane model.

We focus on the role of the DM interaction between the neighbouring spins in a CuO_2 plane. This interaction arises from the orthorhombic distortion in La_2CuO_4 (which is associated with the small tilt of the CuO_6 octahedra) together with the spin-orbit interaction. The DM interaction leads to a small canting of the Cu spins out of the plane, so that the weak ferromagnetic order appears in each CuO_2 plane, and subsequently allows for the formation of 3D AF order. This allows one to observe a pronounced peak in zero-field magnetic susceptibility,[10] $\chi^c(T)$, and the earliest work on the importance of this interaction focused on DM physics. To be specific, Thio *et al.*[3,11] analyzed their susceptibility data using a Landau theory expanded to sixth order, for a 2D Heisenberg antiferromagnet with interlayer coupling and the DM-generated terms. They obtained reasonable fits of their theory to the susceptibility and field dependent magnetization data, and deduced parameters which characterized magnetic properties of the La_2CuO_4 system. As we shall explain below, we believe that the necessity of incorporating such higher-order terms into their fits is suggestive of the important role played by spin-wave interactions, a conclusion consistent with the results presented in this, and our future manuscripts on this problem.

Investigations of the magnetic ground state of La_2CuO_4 were performed by several groups of authors, usually within the framework of the linear spin-wave (SW) theory. The calculations were based on an effective model Hamiltonian derived by Moriya's perturbation theory[8] applied to Hubbard type Hamiltonians by taking into account the spin-orbit coupling. In the most general form, the effective spin Hamiltonian, in addition to the isotropic exchange interaction, includes the abovementioned antisymmetric and symmetric DM interactions. The first microscopic derivation of the spin Hamiltonian was performed by Coffey, Rice, and Zhang;[12] they estimated the antisymmetric DM coupling constants and showed that when the DM vectors alternate a net ferromagnetic moment may be generated in the ground state. Shekhtman, Entin-Wohlman, and Aharony[13] subsequently showed that the symmetric anisotropies contribute to the magnetic energy in the same order as the antisymmetric DM anisotropy, and can never be neglected. Several groups[9,14,15] reexamined the Moriya's theory and found expressions for the effective spin Hamiltonian which includes both types of anisotropies. The linear SW theory applied to such models at $T = 0$ allows one to obtain previously reported values of the spin-wave gaps at the centre of the 2D Brillouin zone, as well as to estimate the magnitudes of the anisotropic-exchange interactions. However, a detailed consideration of the model with the antisymmetric and symmetric DM anisotropies at nonzero temperatures is up to now absent from the literature.

A very rough and simple approximation which can be used to study the effective magnetic model at finite temperatures is the mean field approximation (MFA). The MFA ignores effects of fluctuations and correlations between the spins, hence, it fails for T near T_N and gives no short-range order above the transition temperature. At very low T the noninteracting SW theory is useful, and it gives a successful prediction of the energy of low-lying excited states, and correctly reproduces the dominant term in the low-T magnetization. But, it fails near the phase transition point. To analyze the high temperature behaviour the $1/T$ expansion method can be employed. But, since the La_2CuO_4 crystal ordering temperature is much smaller than the magnitude of the superexchange interaction ($T_N << J$), the high-temperature expansion (to the first few orders in J/T) is not able to discuss the temperature region of interest, that is T near the transition temperature.

In the present paper time we consider the 2D spin-$\frac{1}{2}$ anisotropic quantum Heisenberg antiferromagnet over the entire temperature range including both the symmetric and anti-symmetric DM interactions. We employ the technique of double-time temperature-dependent Green's functions within the framework of the random-phase approximation (RPA). The first time such a scheme was used was by Tyablikov,[16] and he applied this formalism to the Heisenberg ferromagnet (the RPA for magnetic models is often referred to as Tyablikov's decoupling approximation). This work was generalized by Liu[17] to obtain the longitudinal correlation function, and this latter study is important in the development presented in our paper. The important feature of this technique is that it deals with the entire temperature region and is in a good agreement with the SW theory at low-T, as well as with $1/T$ expansions at high-T. In this paper, within such a scheme, we find the transition temperature at which long-range order would be established for an isolated plane. We obtain the excitation spectrum, sublattice magnetization and susceptibility tensor as function of temperature and coupling constants. We also employ the MFA and SW theories to compare results of all of these approximation schemes, and note the essential differences between them.

Of course, many investigations of the 2D spin-$\frac{1}{2}$ have been completed previous to this work. We have already mentioned the most popular and simple methods to study spin models, that is phenomenological Landau theory, linear SW theory, the MFA, and high-temperature expansions. They yield an analytical description of a wide range of physical properties and are very useful for practical purposes. At the same time the great progress in the understanding of the ground state, thermodynamic properties, and spin dynamics of the Heisenberg magnets was made with the use of the newer and more complicated analytical schemes. Arovas and Auerbach[18] used a path-integral formulation of the MFA theory within the Schwinger-boson representation. This method corresponds to the large-N limit of the generalized SU(N) model; however, various difficulties with this method have been discussed in the literature.[19,20] Takahashi[21] has formulated and successfully applied the so-called

modified SW theory to the Heisenberg model which reproduced the results of conventional SW theory and is closely related to the Schwinger-boson theory. For the one dimensional chain, Takahashi's modified SW theory yields very good agreement with Bethe ansatz results, as well as for the 2D classical ferromagnet at low-T (in that it agrees with Monte Carlo results). A self-consistent SW theory that is based on the boson-pseudofermion representation, was developed to study thermodynamics of 2D systems, and was also applied to $S \geq 1$ systems with an Ising-anisotropy 2D magnets.[22] An important feature of all these methods is that they can be used to describe both the ordered and disordered (*i.e.* the case of no long-range order) states.

Other related work includes: (i) The fermion representation to perform a $1/N$ expansion was used by Affleck and Marston,[23] large-S 2D Heisenberg antiferromagnet in the long-wavelength limit; and (ii) based on the diagrammatic method for the spin operators, the thermodynamics and the longitudinal spin dynamics of Heisenberg magnets were studied.[24,25] However, the most note-worthy success in the investigation of this system is the work i of Chakravarty *et al.*[26], who used a renormalization-group approach to the quantum nonlinear σ model, the latter of which describes the low-T behaviour of the 2d Heisenberg AF in the long-wavelength limit.

As will become apparent below, the formalism that we have chosen to implement is more appropriate for this problem than any of those listed above, *or* the theories listed above are too complicated to invoke when one goes beyond the 2D spin-$\frac{1}{2}$ Heisenberg AF and includes spin-orbit couplings.

The above few paragraphs summarize theoretical efforts that were directed towards the understanding of the 2D S=1/2 square lattice AF. The application of these and related work to describe the magnetic properties of so-called single-layer cuprate superconductors, such as La$_2$CuO$_4$, has attracted the attention of many theorists, and fortunately an extensive review of this work, written by Johnston, already exists.[27] In this review[27] one can find the comparison of the temperature dependence of the magnetic susceptibility for an AF Heisenberg square lattice calculated by different analytical methods and quantum Monte Carlo calculations, and, apart from the (post-review) data given by Lavrov *et. al.*[6], the application of the analytical predictions together with the numerical results show very good fitting to the experimental data for the different single-layer cuprate compounds.

Our paper is organized as follows. In §II we present the model Hamiltonian that we will study, introduce a convenient coordinate transformation with which it is simple to complete analytical calculations, and then derive the transformation that relates the static uniform susceptibility in both coordinate systems. In §III we derive and describe the MFA results, and then in §IV we present our derivations from applying the Tyablikov/Liu approach to our model Hamiltonian. In §V we present a detailed ex-

amination of numerical results that follow from our work, including a comparison of MFA, RPA and SW theories. Finally, in §VI we summarize our paper including a brief discussion of the remainder of the work that we have completed on the full three-dimensional problem.

II. MODEL AND DEFINITIONS:

A. Model Hamiltonian and the initial representation

We consider a model for the Cu spins that are present in the CuO$_2$ planes of a La$_2$CuO$_4$ crystal in the low-temperature orthorhombic (LTO) phase and employ a square lattice with nearest-neighbour interactions described by the following effective magnetic Hamiltonian:[13,14]

$$H = J \sum_{\langle i,j \rangle} \mathbf{S}_i \cdot \mathbf{S}_j + \sum_{\langle i,j \rangle} \mathbf{D}_{ij} \cdot (\mathbf{S}_i \times \mathbf{S}_j) + \sum_{\langle i,j \rangle} \mathbf{S}_i \cdot \overleftrightarrow{\Gamma}_{ij} \cdot \mathbf{S}_j. \quad (1)$$

This Hamiltonian consists of the superexchange interaction together with the antisymmetric Dzyaloshinskii-Moriya (DM) interaction (**D** term) and the symmetric pseudodipolar interaction ($\overleftrightarrow{\Gamma}$ term). As was discussed in the introduction, the DM and pseudodipolar anisotropies arise as a result of the mixture of Hubbard-type interaction energies and spin-orbit coupling in the low symmetry crystal structure.

For the LTO phase, we use anisotropic interactions given by of the following form

$$\mathbf{D}_{ab} = \frac{d}{\sqrt{2}}(-1,1,0), \quad \mathbf{D}_{ac} = \frac{d}{\sqrt{2}}(-1,-1,0), \quad (2)$$

and

$$\overleftrightarrow{\Gamma}_{ab} = \begin{pmatrix} \Gamma_1 & \Gamma_2 & 0 \\ \Gamma_2 & \Gamma_1 & 0 \\ 0 & 0 & \Gamma_3 \end{pmatrix}, \quad \overleftrightarrow{\Gamma}_{ac} = \begin{pmatrix} \Gamma_1 & -\Gamma_2 & 0 \\ -\Gamma_2 & \Gamma_1 & 0 \\ 0 & 0 & \Gamma_3 \end{pmatrix}, \quad (3)$$

where the corresponding coordinates, in what we refer to as the "initial representation" in the LTO phase, are shown in Fig. 1(a). Note that the DM vector given in Eq. (2) alternates in sign on successive bonds in the $a-b$ and in the $a-c$ direction of the lattice, as is represented schematically by the double arrows in Fig. 1(b).

We mention that the symmetric tensor $\overleftrightarrow{\Gamma}$ has been obtained by several authors[9,13,14,15,28] in different forms. We have chosen the general form of this tensor, from which other specialized choices can be extracted. For instance, the form of the symmetric tensor obtained by Koshibae, Ohta, and Maekawa[14] can be recovered from this definition if $\Gamma_3 = \Gamma_2 - \Gamma_1$.

In the LTO phase the classical ground state is determined uniquely,[14,15] and below the Néel temperature the Cu spin structure shows long-range antiferromagnetic order with weak ferromagnetism (*viz.* all spins cant out of
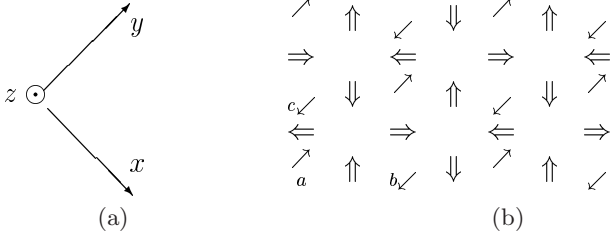
FIG. 1: (a) Coordinates in the initial representation. (b) Thin arrows — the Cu spins, open arrows — the DM vectors.

the plane). To be concrete, in the classical ground state the spins are canted from in-plane antiferromagnetic order by a small angle given by

$$\theta = \frac{1}{2}\tan^{-1}\left(\frac{d/\sqrt{2}}{J + \frac{1}{2}(\Gamma_1 + \Gamma_3)}\right), \qquad (4)$$

and each plane has a net ferromagnetic moment in the z direction perpendicular to the CuO$_2$ planes (weak ferromagnetism).

In the simplified case of the zero pseudodipolar interaction ($\overleftrightarrow{\Gamma} = 0$) it was found[12,29] that the ground-state spin configuration exhibits the rotational symmetry about the DM vector which is the origin of the Goldstone mode in the spin-wave spectrum. Since in this simplified case there is a continuous symmetry in the ground state, the thermal fluctuations destroy the long-range order for any $T > 0$, according to the Mermin and Wagner theorem.[30] In the general case of the model Hamiltonian of Eq. (1), the continuous symmetry no longer exists and the spin-

wave spectrum is gapped in the long wavelength limit $\boldsymbol{q} = 0$. Consequently, *the effect of fluctuations is reduced.* That is, the DM ($\mathbf{D} \neq 0$) together with pseudodipolar ($\overleftrightarrow{\Gamma} \neq 0$) interactions can give rise to long-range order for low (but nonzero) temperatures even for the purely two-dimensional case ($T_N > 0$), and the Mermin and Wagner theorem does not preclude the possibility of a nonzero sublattice magnetization for nonzero temperatures in this general case. (Note that his does not imply that the transition to 3d long-ranged magnetic order is not influenced by the inter-planar exchange coupling, but simply that this latter coupling is not, in general, necessary to achieve such order.)

B. Characteristic representation

In solving this system, it is more convenient (theoretically) to transform from the initial representation, given above, to the characteristic representation (CR) in which the quantization axis (z) is in the direction of a classical moment characterizing the ground state. In the present case there are two such classical vectors in the direction of the canted moments (recall that we are considering only a single CuO$_2$ plane). Therefore, we introduce two rotated coordinate systems, as shown in Fig. 2. Spin degrees of freedom in the initial representation are denoted by $\{S_i\}$, but in the characteristic representation we use $\{\sigma_i\}$. (We follow the notation that i-sites belong to sublattice 1, whereas j-sites belong to sublattice 2.) For the sites of sublattice 1 we apply a transformation of the form

$$
\begin{pmatrix} \sigma_i^x \\ \sigma_i^y \\ \sigma_i^z \end{pmatrix} = \frac{1}{2}\begin{pmatrix} \sin\theta+1 & \sin\theta-1 & -\sqrt{2}\cos\theta \\ \sin\theta-1 & \sin\theta+1 & -\sqrt{2}\cos\theta \\ \sqrt{2}\cos\theta & \sqrt{2}\cos\theta & 2\sin\theta \end{pmatrix}\begin{pmatrix} \frac{1}{\sqrt{2}} & \frac{1}{\sqrt{2}} & 0 \\ \frac{-1}{\sqrt{2}} & \frac{1}{\sqrt{2}} & 0 \\ 0 & 0 & 1 \end{pmatrix}\begin{pmatrix} S_i^x \\ S_i^y \\ S_i^z \end{pmatrix}
$$

$$
= \frac{1}{\sqrt{2}}\begin{pmatrix} 1 & \sin\theta & -\cos\theta \\ -1 & \sin\theta & -\cos\theta \\ 0 & \sqrt{2}\cos\theta & \sqrt{2}\sin\theta \end{pmatrix}\begin{pmatrix} S_i^x \\ S_i^y \\ S_i^z \end{pmatrix}, \qquad (5)
$$

and for sublattice 2

$$
\begin{pmatrix} \sigma_j^x \\ \sigma_j^y \\ \sigma_j^z \end{pmatrix} = \frac{1}{\sqrt{2}}\begin{pmatrix} 1 & \sin\theta & \cos\theta \\ -1 & \sin\theta & \cos\theta \\ 0 & -\sqrt{2}\cos\theta & \sqrt{2}\sin\theta \end{pmatrix}\begin{pmatrix} S_j^x \\ S_j^y \\ S_j^z \end{pmatrix}. \qquad (6)
$$

The quantization axes (z) of the new spin operators σ_i and σ_j coincide with the unit vectors in the direction of canted moments moments Fig. 2.

The model Hamiltonian of Eq. (1) in terms of the new operators σ reads

$$
\begin{aligned}
H_{\mathrm{CR}} = &\sum_{\langle i,j\rangle_{ab}} \Big\{ A(\sigma_i^+\sigma_j^- + \sigma_i^-\sigma_j^+) - B^*\sigma_i^+\sigma_j^+ \\
&\qquad\qquad - B\sigma_i^-\sigma_j^- - J_2\sigma_i^z\sigma_j^z \Big\} \\
+ &\sum_{\langle i,j\rangle_{ac}} \Big\{ A(\sigma_i^+\sigma_j^- + \sigma_i^-\sigma_j^+) + B\sigma_i^+\sigma_j^+ \\
&\qquad\qquad + B^*\sigma_i^-\sigma_j^- - J_2\sigma_i^z\sigma_j^z \Big\},
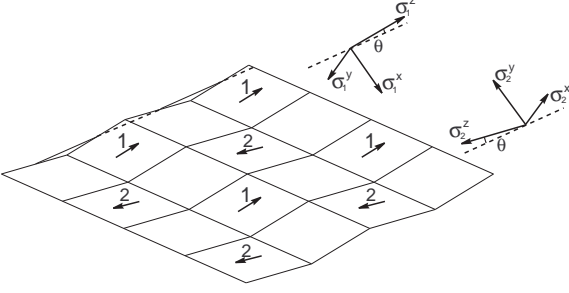\end{aligned} \qquad (7)
$$

FIG. 2: Numbered arrows represent the Cu spin structure in a CuO$_2$ plane. Two sublattices 1 and 2 are introduced. For each sublattice the spin coordinate system within the characteristic representation (*i.e.* after the transformations given by (5) and (6)) is shown. The thin net is shown only to simplify the visualization of the spin structure.

where we introduced the following definitions

$$J_1 = J + \Gamma_1,$$

$$J_2 = \frac{1}{2}(\Gamma_1 - \Gamma_3) + \sqrt{(d^2/2) + [J + \frac{1}{2}(\Gamma_1 + \Gamma_3)]^2},$$

$$J_3 = -\frac{1}{2}(\Gamma_1 - \Gamma_3) + \sqrt{(d^2/2) + [J + \frac{1}{2}(\Gamma_1 + \Gamma_3)]^2},$$

$$J_4 = -\Gamma_2 \sin\theta + \frac{d}{\sqrt{2}}\cos\theta,$$

$$\tag{8}$$

$$A = \frac{J_1 - J_3}{4}, \qquad B = \frac{J_4}{2} + \mathrm{i}\frac{J_1 + J_3}{4}. \tag{9}$$

The subscripts $\langle i,j \rangle_{ab}$ and $\langle i,j \rangle_{ac}$ in the summations of Eq. (7) imply the nearest neighbours in the ab and ac directions, as shown in Fig. 1(b).

The form of the Hamiltonian in the characteristic representation is similar to an XYZ model, but is clearly more complicated since terms of the form $\sigma_i^- \sigma_j^- - \sigma_i^+ \sigma_j^+$ are present, which thus imply terms like $S_i^x S_j^y$. Thus, we can extract from our results, in this representation, the magnetic susceptibility of the XYZ calculated in both the mean-field and random phase approximations, by setting the imaginary part $B = 0$. We will consider numerical results for this simpler model in a future publication.

C. Magnetic susceptibility in the initial and characteristic representations

We consider the response of the system, described by the Hamiltonian H in either the initial (Eq. (1)) or characteristic representation (Eq. (7)), to an externally applied constant magnetic field **h**. It is convenient to consider the application of this field in one direction only, which we take to be the α direction *of the initial repre-*

sentation,

$$H' = H - h^\alpha \sum_{l=1}^N S_l^\alpha, \tag{10}$$

where $\alpha = x$ or y or z, it is to be noted that α is not summer over in Eq. (10), and N is the number of the lattice sites.

The statistical operator of the system is required to evaluate ensemble averages of relevant physical quantities, notably correlators and thermal Green's functions, and can be written as

$$\rho = \mathrm{e}^{-\beta H'} = \mathrm{e}^{-\beta H} T_\tau \exp\left\{ h^\alpha \sum_{l=1}^N \int_0^\beta S_l^\alpha(\tau)\mathrm{d}\tau \right\}, \tag{11}$$

where $S_l(\tau) = \mathrm{e}^{H\tau} S_l \mathrm{e}^{-H\tau}$ is the operator in the Heisenberg representation for imaginary time argument τ, and T_τ is the time-ordering operator. The zero-field susceptibility describes the response of the system to such a field, and is defined to be

$$\chi^\alpha \equiv \left.\frac{\partial \langle M^\alpha \rangle}{\partial h^\alpha}\right|_{h^\alpha = 0} = \frac{1}{N}\sum_{l=1}^N \sum_{l'=1}^N \int_0^\beta \langle T_\tau S_l^\alpha(\tau) S_{l'}^\alpha(0)\rangle\mathrm{d}\tau,$$

$$\tag{12}$$

where

$$\langle M^\alpha \rangle = 1/N \sum_l^N \langle S_l^\alpha \rangle, \tag{13}$$

with correlators such as $\langle T_\tau S_l^\alpha(\tau) S_{l'}^\alpha(0)\rangle$ taken with respect to the zero field Hamiltonian H.

The square lattice is bipartite and can be divided into sublattices 1 and 2. Then, by using the definitions

$$\chi_{11}^\alpha = \frac{2}{N}\sum_{i=1}^{N/2}\sum_{i'=1}^{N/2}\int_0^\beta \langle T_\tau S_i^\alpha(\tau) S_{i'}^\alpha(0)\rangle\mathrm{d}\tau, \tag{14}$$

$$\chi_{22}^\alpha = \frac{2}{N}\sum_{j=1}^{N/2}\sum_{j'=1}^{N/2}\int_0^\beta \langle T_\tau S_j^\alpha(\tau) S_{j'}^\alpha(0)\rangle\mathrm{d}\tau, \tag{15}$$

$$\chi_{12}^\alpha = \frac{2}{N}\sum_{i=1}^{N/2}\sum_{j=1}^{N/2}\int_0^\beta \langle T_\tau S_i^\alpha(\tau) S_j^\alpha(0)\rangle\mathrm{d}\tau, \tag{16}$$

$$\chi_{21}^\alpha = \frac{2}{N}\sum_{j=1}^{N/2}\sum_{i=1}^{N/2}\int_0^\beta \langle T_\tau S_j^\alpha(\tau) S_i^\alpha(0)\rangle\mathrm{d}\tau, \tag{17}$$

where

$$i, i' \in \text{ sublattice } 1, \quad j, j' \in \text{ sublattice } 2$$

we can express the quantity of interest, χ^α, as

$$\chi^\alpha = \frac{1}{2}\{\chi_{11}^\alpha + \chi_{22}^\alpha + \chi_{12}^\alpha + \chi_{21}^\alpha\}. \tag{18}$$

Then, using symmetry equivalent this simplifies (see below) the calculation of the zero-field susceptibility in the initial representation to

$$\chi^\alpha = \chi_{11}^\alpha + \chi_{12}^\alpha. \tag{19}$$

The simpler form of Eq. (7) *vs.* Eq. (1) makes clear that it is desirable to perform calculations first using the characteristic representation, and to then transform back into the initial representation. To this end we require the relevant form of the susceptibility tensor in the characteristic representation. To begin, let us perform transformations $\mathbf{S}_1 = \mathcal{A}\boldsymbol{\sigma}_1$, $\mathbf{S}_2 = \mathcal{B}\boldsymbol{\sigma}_2$ ($\mathcal{A} = [a_{\alpha\alpha'}]$, $\mathcal{B} = [b_{\alpha\alpha'}]$) to the characteristic representation, such that the analogue of Eq. (10) is

$$H' = H_{\mathrm{CR}} \;-\; \sum_{i=1}^{N/2}(a_{\alpha x}\sigma_i^x + a_{\alpha y}\sigma_i^y + a_{\alpha z}\sigma_i^z)h_1^\alpha$$
$$-\; \sum_{j=1}^{N/2}(b_{\alpha x}\sigma_j^x + b_{\alpha y}\sigma_j^y + b_{\alpha z}\sigma_j^z)h_2^\alpha. \tag{20}$$

Note that we have generalized the applied field to be $\mathbf{h_1}$ for sublattice 1, and $\mathbf{h_2}$ for sublattice 2, and in general we will treat these as two independent applied fields. If we define the components of susceptibility in the characteristic representation as

$$\chi_{11}^{\sigma^\alpha\sigma^{\alpha'}} = \frac{2}{N}\sum_{i=1}^{N/2}\sum_{i'=1}^{N/2}\int_0^\beta \langle T_\tau \sigma_i^\alpha(\tau)\sigma_{i'}^{\alpha'}(0)\rangle \mathrm{d}\tau, \tag{21}$$

$$\chi_{12}^{\sigma^\alpha\sigma^{\alpha'}} = \frac{2}{N}\sum_{i=1}^{N/2}\sum_{j=1}^{N/2}\int_0^\beta \langle T_\tau \sigma_i^\alpha(\tau)\sigma_j^{\alpha'}(0)\rangle \mathrm{d}\tau, \tag{22}$$

then the susceptibility given in Eq. (14) (*N.B.* in the initial representation) can be written as

$$\begin{aligned}
\chi_{11}^\alpha &= \frac{2}{N}\sum_{i=1}^{N/2}\frac{\partial\langle S_i^\alpha\rangle}{\partial h_1^\alpha}\\
&= \frac{2}{N}\sum_{i=1}^{N/2}\left\{a_{\alpha x}\frac{\partial\langle\sigma_i^x\rangle}{\partial h_1^\alpha} + a_{\alpha y}\frac{\partial\langle\sigma_i^y\rangle}{\partial h_1^\alpha} + a_{\alpha z}\frac{\partial\langle\sigma_i^z\rangle}{\partial h_1^\alpha}\right\}\\
&= a_{\alpha x}^2\chi_{11}^{\sigma^x\sigma^x} + a_{\alpha x}a_{\alpha y}\chi_{11}^{\sigma^x\sigma^y} + a_{\alpha x}a_{\alpha z}\chi_{11}^{\sigma^x\sigma^z}\\
&+ a_{\alpha y}^2\chi_{11}^{\sigma^y\sigma^y} + a_{\alpha y}a_{\alpha x}\chi_{11}^{\sigma^y\sigma^x} + a_{\alpha y}a_{\alpha z}\chi_{11}^{\sigma^y\sigma^z}\\
&+ a_{\alpha z}^2\chi_{11}^{\sigma^z\sigma^z} + a_{\alpha z}a_{\alpha x}\chi_{11}^{\sigma^z\sigma^x} + a_{\alpha z}a_{\alpha y}\chi_{11}^{\sigma^z\sigma^y},
\end{aligned} \tag{23}$$

and, in the same way (see Eq. (19))

$$\begin{aligned}
\chi_{12}^\alpha &= a_{\alpha x}b_{\alpha x}\chi_{12}^{\sigma^x\sigma^x} + a_{\alpha x}b_{\alpha y}\chi_{12}^{\sigma^x\sigma^y} + a_{\alpha x}b_{\alpha z}\chi_{12}^{\sigma^x\sigma^z}\\
&+ a_{\alpha y}b_{\alpha y}\chi_{12}^{\sigma^y\sigma^y} + a_{\alpha y}b_{\alpha x}\chi_{12}^{\sigma^y\sigma^x} + a_{\alpha y}b_{\alpha z}\chi_{12}^{\sigma^y\sigma^z}\\
&+ a_{\alpha z}b_{\alpha z}\chi_{12}^{\sigma^z\sigma^z} + a_{\alpha z}b_{\alpha x}\chi_{12}^{\sigma^z\sigma^x} + a_{\alpha z}b_{\alpha y}\chi_{12}^{\sigma^z\sigma^y}.
\end{aligned} \tag{24}$$

The quantities $\chi^{\sigma^\alpha\sigma^{\alpha'}}$ that are introduced above in Eqs. (21,22) have the following interpretation. For instance, the component $\chi_{12}^{\sigma^\alpha\sigma^{\alpha'}}$ determine the response of the expectation value $2/N\sum_{i=1}^{N/2}\langle\sigma_i^\alpha\rangle$ of the spins of sublattice 1 to the magnetic field applied to the spins sublattice 2 (no field applied to the spins of sublattice 1) in the α' direction. Indeed, the perturbation $H' = H - h_2^{\alpha'}\sum_{j=1}^{N/2}\sigma_j^{\alpha'}$ formally leads to the response

$$\frac{2}{N}\frac{\partial}{\partial h_2^{\alpha'}}\sum_{i=1}^{N/2}\langle\sigma_i^\alpha\rangle = \frac{2}{N}\sum_{i=1}^{N/2}\sum_{j=1}^{N/2}\int_0^\beta\langle T_\tau\sigma_i^\alpha(\tau)\sigma_j^{\alpha'}(0)\rangle\mathrm{d}\tau \equiv \chi_{12}^{\sigma^\alpha\sigma^{\alpha'}}. \tag{25}$$

Similarly, the response of the spins of sublattice 1 to the perturbation $H' = H - h_1^{\alpha'}\sum_{i=1}^{N/2}\sigma_i^{\alpha'}$ is given by

$$\frac{2}{N}\frac{\partial}{\partial h_1^{\alpha'}}\sum_{i=1}^{N/2}\langle\sigma_i^\alpha\rangle = \frac{2}{N}\sum_{i=1}^{N/2}\sum_{i'=1}^{N/2}\int_0^\beta\langle T_\tau\sigma_i^\alpha(\tau)\sigma_{i'}^{\alpha'}(0)\rangle\mathrm{d}\tau \equiv \chi_{11}^{\sigma^\alpha\sigma^{\alpha'}}. \tag{26}$$

So, by substituting the inverse to the CR transformation, given by Eqs. (5,6), into Eqs. (23,24), and taking into account that $\chi^{\sigma^x\sigma^z} = \chi^{\sigma^y\sigma^z} = \chi^{\sigma^z\sigma^x} = \chi^{\sigma^z\sigma^y} = 0$ in the

characteristic representation (which can be derived analytically), one obtains the desired transformation between the two representations, namely

$$\chi^x = \chi_{11}^x + \chi_{12}^x \; = \; \frac{1}{2}(\chi_{11}^{\sigma^x\sigma^x} + \chi_{12}^{\sigma^x\sigma^x} + \chi_{11}^{\sigma^y\sigma^y} + \chi_{12}^{\sigma^y\sigma^y} - \chi_{11}^{\sigma^x\sigma^y} - \chi_{12}^{\sigma^x\sigma^y} - \chi_{11}^{\sigma^y\sigma^x} - \chi_{12}^{\sigma^y\sigma^x}), \tag{27}$$

$$\chi^y = \chi_{11}^y + \chi_{12}^y \; = \; \frac{\sin^2(\theta)}{2}(\chi_{11}^{\sigma^x\sigma^x} + \chi_{12}^{\sigma^x\sigma^x} + \chi_{11}^{\sigma^y\sigma^y} + \chi_{12}^{\sigma^y\sigma^y} + \chi_{11}^{\sigma^x\sigma^y} + \chi_{12}^{\sigma^x\sigma^y} + \chi_{11}^{\sigma^y\sigma^x} + \chi_{12}^{\sigma^y\sigma^x})$$
$$+ \cos^2(\theta)(\chi_{11}^{\sigma^z\sigma^z} - \chi_{12}^{\sigma^z\sigma^z}), \tag{28}$$

$$\chi^z = \chi_{11}^z + \chi_{12}^z \; = \; \frac{\cos^2(\theta)}{2}(\chi_{11}^{\sigma^x\sigma^x} - \chi_{12}^{\sigma^x\sigma^x} + \chi_{11}^{\sigma^y\sigma^y} - \chi_{12}^{\sigma^y\sigma^y} + \chi_{11}^{\sigma^x\sigma^y} - \chi_{12}^{\sigma^x\sigma^y} + \chi_{11}^{\sigma^y\sigma^x} - \chi_{12}^{\sigma^y\sigma^x})$$
$$+ \sin^2(\theta)(\chi_{11}^{\sigma^z\sigma^z} + \chi_{12}^{\sigma^z\sigma^z}). \tag{29}$$

III. MEAN FIELD ANALYSIS

In this section we develop the mean field approximation (MFA) for the system defined by Eq. (1), and obtain the behaviour of the magnetic susceptibility and a defining equation for the order parameter as a function of temperature. In part we include this derivation to make evident how the formalism of § II C is applied to extract the zero-field uniform magnetic susceptibility. However, and more importantly, we will show that when the canting angle induced by the DM couplings is small, there are significant deviations from the mean-field results, *viz.* quantum fluctuation effects are large. Thus, here we establish the MFA susceptibility with which to make these comparisons.

Within the MFA we focus on one of the spins and replace its interaction with other spins by an effective field. To this end the following replacement is used:

$$S_i^a S_j^b = \langle S_i^a \rangle \, S_j^b \; + \; S_i^a \, \langle S_j^b \rangle \; - \; \langle S_i^a \rangle \, \langle S_j^b \rangle, \tag{30}$$

where a and b can be equal to any of x, y, z. It is to be noted that it is more convenient to perform the MFA calculations starting from the model in the characteristic representation, and thus we consider Eq. (7) and the analogue of the above equation for the σ operators.

First, we find the equation for the order parameter. The Hamiltonian Eq. (7) within the MFA reads as

$$H_i^{MFA} = -\mathcal{Z}J_2 \langle \sigma^z \rangle \sigma_i^z, \tag{31}$$

and we find that the order parameter, to be denoted by η, is found from the solution of

$$\eta \equiv \langle \sigma^z \rangle = \frac{1}{2} \tanh \left\{ \frac{\beta}{2} \mathcal{Z}J_2 \langle \sigma^z \rangle \right\}, \tag{32}$$

where J_2 is given by Eq. (8), and $\mathcal{Z}$ is the coordination number. From this equation it is immediately seen that within the MFA the Néel temperature at which η vanishes is

$$T_N^{MFA} = J_2 = \frac{1}{2}(\Gamma_1 - \Gamma_3) + \sqrt{(d^2/2) + [J + \frac{1}{2}(\Gamma_1 + \Gamma_3)]^2} \tag{33}$$

Now, we find the susceptibility of the system within the MFA below T_N^{MFA}. First, we apply a magnetic field in the z direction of the sublattice 1

$$H' = H - h_1^z \sum_i \sigma_i^z, \quad i\text{-sites} \in 1 \text{ sublattice}. \tag{34}$$

The Hamiltonian within the MFA can be written as

$$H'^{\,MFA} = -\sum_i \left(\sum_{\langle j \rangle_i} J_2 \langle \sigma_j^z \rangle + h_1^z \right) \sigma_i^z - \sum_j \sum_{\langle i \rangle_j} J_2 \langle \sigma_i^z \rangle \sigma_j^z, \tag{35}$$

where $\sum_{\langle i \rangle_j}$ means sum over all sites i which are nearest neighbours of site j. Then

$$\langle \sigma_i^z \rangle \; = \; \frac{1}{2} \tanh \left\{ \frac{\beta}{2} \left(\sum_{\langle j \rangle_i} J_2 \langle \sigma_j^z \rangle + h_1^z \right) \right\},$$
$$\langle \sigma_j^z \rangle \; = \; \frac{1}{2} \tanh \left\{ \frac{\beta}{2} \sum_{\langle i \rangle_j} J_2 \langle \sigma_i^z \rangle \right\}. \tag{36}$$

We write the mean value of σ^z operators in the form

$$\langle \sigma_i^z \rangle = \langle \sigma_1^z \rangle_0 + \delta\sigma_1^z, \; \langle \sigma_j^z \rangle = \langle \sigma_2^z \rangle_0 + \delta\sigma_2^z, \tag{37}$$

where $\langle \sigma_1^z \rangle_0 = \langle \sigma_2^z \rangle_0 = \eta$, is the expectation value of σ^z operator in the absence of the field, and the term $\delta\sigma^z$ is the part of $\langle \sigma^z \rangle$ induced by the applied field. Since the applied field h_1^z as well as the terms involving $\delta\sigma^z$ are small, we may expand Eq. (36) in powers of these terms. Then, we find

$$\chi_{11}^{\sigma^z\sigma^z} = \left. \frac{\delta\sigma_1^z}{h_1^z} \right|_{h_1^z=0} = \frac{\frac{\beta}{4}\mathrm{sech}^2\left\{\frac{\beta}{2}\mathcal{Z}J_2\eta\right\}}{1-(\frac{\beta J_2 \mathcal{Z}}{4})^2\mathrm{sech}^4\left\{\frac{\beta}{2}\mathcal{Z}J_2\eta\right\}},$$

$$\chi_{21}^{\sigma^z\sigma^z} = \left. \frac{\delta\sigma_2^z}{h_1^z} \right|_{h_1^z=0} = \frac{\mathcal{Z}J_2(\frac{\beta}{4})^2\mathrm{sech}^4\left\{\frac{\beta}{2}\mathcal{Z}J_2\eta\right\}}{1-(\frac{\beta J_2 \mathcal{Z}}{4})^2\mathrm{sech}^4\left\{\frac{\beta}{2}\mathcal{Z}J_2\eta\right\}}. \tag{38}$$

Due to the complicated couplings found in Eq. (7), the transverse components are much more involved to

calculate. Applying a field in the x direction to the spins of sublattice 1 we consider

$$H' = H - h_1^x \sum_i \sigma_i^x, \quad i\text{-sites} \in 1\text{-sublattice}, \qquad (39)$$

and within the MFA we thus examine

$$H'^{\ MFA} = -\sum_i ([\mathfrak{h}_1^x + h_1^x]\sigma_i^x + \mathfrak{h}_1^y \sigma_i^y + \mathfrak{h}_1^z \sigma_i^z)$$
$$- \sum_j (\mathfrak{h}_2^x \sigma_j^x + \mathfrak{h}_2^y \sigma_j^y + \mathfrak{h}_2^z \sigma_j^z). \qquad (40)$$

Similarly, by applying a field in the y direction to the spins of sublattice 1 we consider

$$H'^{\ MFA} = -\sum_i (\mathfrak{h}_1^x \sigma_i^x + [\mathfrak{h}_1^y + h_1^y]\sigma_i^y + \mathfrak{h}_1^z \sigma_i^z)$$
$$- \sum_j (\mathfrak{h}_2^x \sigma_j^x + h_2^y \sigma_j^y + \mathfrak{h}_2^z \sigma_j^z), \qquad (41)$$

where

$$\mathfrak{h}_1^x = \sum_{\langle j \rangle_i} \{-2A\langle \sigma_j^x \rangle + 2\Im B\langle \sigma_j^y \rangle\},$$

$$\mathfrak{h}_2^x = \sum_{\langle i \rangle_j} \{-2A\langle \sigma_i^x \rangle + 2\Im B\langle \sigma_i^y \rangle\},$$

$$\mathfrak{h}_1^y = \sum_{\langle j \rangle_i} \{-2A\langle \sigma_j^y \rangle + 2\Im B\langle \sigma_j^x \rangle\},$$

$$\mathfrak{h}_2^y = \sum_{\langle i \rangle_j} \{-2A\langle \sigma_i^y \rangle + 2\Im B\langle \sigma_i^x \rangle\},$$

$$\mathfrak{h}_1^z = \sum_{\langle j \rangle_i} J_2 \langle \sigma_j^z \rangle, \quad \mathfrak{h}_2^z = \sum_{\langle i \rangle_j} J_2 \langle \sigma_i^z \rangle,$$

where $\Im B$ denotes the imaginary part of B. Then, the system of equations determining the transverse components of susceptibility Eq. (25) and Eq. (26) within the MFA scheme is found to be

$$-\frac{J_2}{2}\chi_{11}^{\sigma^x \sigma^x} = A\chi_{21}^{\sigma^x \sigma^x} - \Im B\chi_{21}^{\sigma^y \sigma^x} - \frac{1}{2\mathcal{Z}},$$

$$-\frac{J_2}{2}\chi_{21}^{\sigma^x \sigma^x} = A\chi_{11}^{\sigma^x \sigma^x} - \Im B\chi_{11}^{\sigma^y \sigma^x},$$

$$-\frac{J_2}{2}\chi_{11}^{\sigma^y \sigma^x} = A\chi_{21}^{\sigma^y \sigma^x} - \Im B\chi_{21}^{\sigma^x \sigma^x},$$

$$-\frac{J_2}{2}\chi_{21}^{\sigma^y \sigma^x} = A\chi_{11}^{\sigma^y \sigma^x} - \Im B\chi_{11}^{\sigma^x \sigma^x},$$

$$-\frac{J_2}{2}\chi_{11}^{\sigma^x \sigma^y} = A\chi_{21}^{\sigma^x \sigma^y} - \Im B\chi_{21}^{\sigma^y \sigma^y},$$

$$-\frac{J_2}{2}\chi_{21}^{\sigma^x \sigma^y} = A\chi_{11}^{\sigma^x \sigma^y} - \frac{\mathcal{Z}}{4}\Im B\chi_{11}^{\sigma^y \sigma^y},$$

$$-\frac{J_2}{2}\chi_{11}^{\sigma^y \sigma^y} = A\chi_{21}^{\sigma^y \sigma^y} - \Im B\chi_{21}^{\sigma^x \sigma^y} - \frac{1}{2\mathcal{Z}},$$

$$-\frac{J_2}{2}\chi_{21}^{\sigma^y \sigma^y} = A\chi_{11}^{\sigma^y \sigma^y} - \Im B\chi_{11}^{\sigma^x \sigma^y}. \qquad (42)$$

The solution of this systems, Eq. (42) turns out to be

$$\chi_{11}^{\sigma^x \sigma^x} = \chi_{22}^{\sigma^x \sigma^x} = \chi_{11}^{\sigma^y \sigma^y} = \chi_{22}^{\sigma^y \sigma^y} = \frac{J_2/2+A}{4\mathcal{Z}\omega_1^2} + \frac{J_2/2-A}{4\mathcal{Z}\omega_2^2},$$

$$\chi_{12}^{\sigma^x \sigma^x} = \chi_{21}^{\sigma^x \sigma^x} = \chi_{12}^{\sigma^y \sigma^y} = \chi_{21}^{\sigma^y \sigma^y} = \frac{J_2/2+A}{\omega_1^2} - \frac{J_2/2-A}{4\mathcal{Z}\omega_2^2},$$

$$\chi_{11}^{\sigma^x \sigma^y} = \chi_{22}^{\sigma^x \sigma^y} = \chi_{11}^{\sigma^y \sigma^x} = \chi_{22}^{\sigma^y \sigma^x} = \frac{\Im B}{4\mathcal{Z}}\left(\frac{1}{\omega_1^2} - \frac{1}{\omega_2^2}\right),$$

$$\chi_{12}^{\sigma^x \sigma^y} = \chi_{21}^{\sigma^x \sigma^y} = \chi_{12}^{\sigma^y \sigma^x} = \chi_{21}^{\sigma^y \sigma^x} = \frac{\Im B}{4\mathcal{Z}}\left(\frac{1}{\omega_1^2} + \frac{1}{\omega_2^2}\right),$$
$$(43)$$

where

$$\omega_1 = \sqrt{(J_2/2 + A)^2 - \Im B^2},$$
$$\omega_2 = \sqrt{(J_2/2 - A)^2 - \Im B^2}.$$
$$(44)$$

Using the relation between the components of susceptibility in the initial and characteristic representations given in Eqs. (27)-(29), we obtain the final result for zero-field uniform susceptibility within the MFA below the MFA ordering temperature, T_N^{MFA}, viz.

$$\chi^{x\ MFA} = \frac{1}{4}\frac{1}{J_1 + J_2}, \qquad (45)$$

$$\chi^{y\ MFA} = \frac{1}{4}\frac{\sin^2(\theta)}{J_2 - J_3} + \frac{\cos^2(\theta)}{4}\frac{\text{sech}^2\left\{\frac{\beta}{2}zJ_2\eta\right\}}{T + J_2\ \text{sech}^2\left\{\frac{\beta}{2}zJ_2\eta\right\}}, \qquad (46)$$

$$\chi^{z\ MFA} = \frac{1}{4}\frac{\cos^2(\theta)}{J_2 + J_3} + \frac{\sin^2(\theta)}{4}\frac{\text{sech}^2\left\{\frac{\beta}{2}zJ_2\eta\right\}}{T - J_2\ \text{sech}^2\left\{\frac{\beta}{2}zJ_2\eta\right\}}, \qquad (47)$$

with the equation for the order parameter η given by Eq. (32). (For $d = \Gamma_i = 0$, implying that $\theta = 0$ and $J_2 = J$, the above seemingly complicated results indeed reduce to the correct MFA expression for the susceptibility.)

The following comments on the MFA result are in order. First, note that for physical values of d and Γ_i (d, $\Gamma_i \ll J$) the canting angle out of the xy plane is very small; thus, since the AF moment is in the yz plane and nearly aligned along the $\pm y$ axes, χ^z diverges at T_N^{MFA}, but the other two components remain finite at the transition. However, while the x component of the susceptibility remains independent of temperature, since the canting produces a net FM moment in the z direction that is coupled to the y component of the local moment, there is an additional increase of χ^y as the transition is approached from below.

Now consider the paramagnetic temperature region ($T > T_N$), for which the only components with nonzero spin expectation values are those driven by the applied

field. Following similar considerations to above, the final results for the components of susceptibility in the initial representation for high temperatures $(T > T_N)$ reads

$$\chi^{x\ MFA} = \frac{1}{4}\frac{1}{J_1 + T}, \tag{48}$$

$$\chi^{y\ MFA} = \frac{1}{4}\frac{\sin^2(\theta)}{T - J_3} + \frac{1}{4}\frac{\cos^2(\theta)}{T + J_2}, \tag{49}$$

$$\chi^{z\ MFA} = \frac{1}{4}\frac{\cos^2(\theta)}{T + J_3} + \frac{1}{4}\frac{\sin^2(\theta)}{T - J_2}. \tag{50}$$

Note that in the limit $T \to T_N^{MFA} = J_2$ we obtain that the x, y components of the susceptibility are continuous at the transition, whereas the z component of the susceptibility diverges at the Néel point, from above or below, owing to the presence of the weak ferromagnetic moment that first develops at the transition.

IV. LINEAR RESPONSE THEORY WITHIN THE RPA

A. Susceptibility below T_N

In this section we derive expressions for the static, uniform susceptibility within the RPA below the ordering temperature, T_N. Note that this temperature is determined with the RPA, and is not equivalent to that found in the previous section.

We employ thermal Green's functions in the analysis of the spin Hamiltonian given in Eq. (1) with spin $\frac{1}{2}$. The definition of such Green's functions for two Bose operators A, B and the corresponding equation of motion, are given by

$$G_{AB}(\tau) = \langle T_\tau A(\tau)B(0)\rangle, \tag{51}$$

$$\frac{dG_{AB}(\tau)}{d\tau} = \delta(\tau)\langle[A, B]\rangle + \langle T_\tau[H(\tau), A(\tau)]B(0)\rangle. \tag{52}$$

As discussed in the introduction, we adopt a procedure that was introduced by Liu,[17] as this technique allows for us to find longitudinal component of the susceptibility. To this end, we introduce the perturbed Hamiltonian (in the characteristic representation)

$$H_1^f = H_{CR} - f\sum_i \sigma_i^z, \tag{53}$$

where f is a small fictitious field; note that the field is

applied to the spins of *sublattice 1 only*, and within the present paper we restrict f to be constant and static.

In the imaginary-time formalism, the Green's functions to be used are

$$G_{ln}^f(\tau) = \langle T_\tau \sigma_l^+(\tau)\sigma_n^-(0)\rangle^f,$$
$$G_{ln}^{f-}(\tau) = \langle T_\tau \sigma_l^-(\tau)\sigma_n^-(0)\rangle^f,\ l \in \text{sublattice 1},$$
$$G_{n'n}^f(\tau) = \langle T_\tau \sigma_{n'}^+(\tau)\sigma_n^-(0)\rangle^f,$$
$$G_{n'n}^{f-}(\tau) = \langle T_\tau \sigma_{n'}^-(\tau)\sigma_n^-(0)\rangle^f,\ n \in \text{sublattice 2},$$
$$\tag{54}$$

where the expectation values are taken with respect to the perturbed Hamiltonian in Eq. (53). After an expansion in a power series of f we can write

$$G_{ln}^f(\tau) = G_{ln}^{(0)}(\tau) + fG_{ln}^{(1)}(\tau) + O(f^2). \tag{55}$$

Since $G_{ln}^{(0)}(\tau) = G_{ln}(\tau)$, from now drop the superscript and use

$$G_{ln}^f(\tau) = G_{ln}(\tau) + fG_{ln}^{(1)}(\tau) + O(f^2). \tag{56}$$

Also, we introduce

$$\langle \sigma_i^z(\tau)\rangle^f = \langle\sigma_i^z\rangle + fv_i + O(f^2), \tag{57}$$

where, due to the translation periodicity $\langle\sigma_i^z\rangle = \eta$, the order parameter at $f = 0$.

The equation of motion for the Green's function $G_{ln}^f(\tau)$ is given by

$$\frac{dG_{ln}^f(\tau)}{d\tau} = 2\delta(\tau)\delta_{ln}\langle\sigma_l^z\rangle^f$$
$$+ \langle T_\tau[H_{CR}(\tau), \sigma_l^+(\tau)]\sigma_n^-(0)\rangle^f - fG_{ln}^f. \tag{58}$$

In order to solve this equation for the Green's function it must be linearized. We will use the random phase approximation (RPA), in which the fluctuations of σ^z are ignored and the operator σ^z is replaced by its mean value $\langle\sigma^z\rangle^f$ — this is the so-called Tyablikov's decoupling.[16] For example

$$\langle T_\tau\sigma_l^z(\tau)\sigma_i^+(\tau)\sigma_j^-(0)\rangle^f \to$$
$$\to \langle\sigma_l^z(\tau)\rangle^f\langle T_\tau\sigma_i^+(\tau)\sigma_j^-(0)\rangle^f = \langle\sigma_l^z(\tau)\rangle^f G_{ij}^f(\tau). \tag{59}$$

After this decoupling is introduced, Eq. (58) is found to be

$$\frac{dG_{ln}^f(\tau)}{d\tau} = 2\delta(\tau)\delta_{ln}\langle\sigma_l^z\rangle^f - \sum_{\delta_{ab}}\left\{2\langle\sigma_l^z(\tau)\rangle^f[AG_{(l+\delta)n}^f(\tau) - BG_{(l+\delta)n}^{f-}(\tau)] + J_2\langle\sigma_{l+\delta}^z(\tau)\rangle^f G_{ln}^f(\tau)\right\}$$

$$- \sum_{\delta_{ac}}\left\{2\langle\sigma_l^z(\tau)\rangle^f[AG_{(l+\delta)n}^f(\tau) + B^*G_{(l+\delta)n}^{f-}(\tau)] + J_2\langle\sigma_{l+\delta}^z(\tau)\rangle^f G_{ln}^f(\tau)\right\} - fG_{ln}^f(\tau), \tag{60}$$

where $\sum_{\delta_{ab}}$ refers to a summation over the nearest neighbours of the site l in the ab direction, and similarly for $\sum_{\delta_{ac}}$ — see Fig. 1(b). Here, all sites $l + \delta$ belong to the sublattice 2.

We introduce the Fourier transformation in the momentum-frequency representation for the Green's function and the spin operator

$$G_{ln}^{f}(\tau) = \frac{2}{N\beta} \sum_{\boldsymbol{k},m} G_{12}^{f}(\boldsymbol{k}, \omega_m) e^{i\boldsymbol{k}\cdot(\mathbf{R}_l - \mathbf{R}_n)} e^{-i\omega_m \tau}, \quad (61)$$

$$\begin{aligned} \langle \sigma_l^z(\tau) \rangle^f &= \frac{1}{\beta} \sum_{\boldsymbol{k},m} \langle \sigma_1^z(\boldsymbol{k}, \omega_m) \rangle^f e^{-i\boldsymbol{k}\cdot\mathbf{R}_l} e^{-i\omega_m \tau} \\ &= \sum_{\boldsymbol{k}} \delta(\boldsymbol{k})[\eta + f\mathrm{v}_1] e^{-i\boldsymbol{k}\cdot\mathbf{R}_l}, \quad (62) \end{aligned}$$

where the expansion in Eq. (57) and the linear response to the uniform perturbation expressed by $\mathrm{v}_1(\boldsymbol{k}) = \delta(\boldsymbol{k})\mathrm{v}_1$ were taken into account. In the transformation given by Eqs. (61,62), the sum over $\boldsymbol{k}$ runs over $\frac{1}{2}N$ points of the first zone in the momentum space, and $\omega_n = 2\pi n/\beta$ for $n \in \mathbb{Z}$ are the Bose Matsubara frequencies. Then, we can write down the equation for the Green's function $G_{ln}^{f}(\tau)$ in the form

$$\begin{aligned} -i\omega_m G_{12}^{f}(\boldsymbol{k}, \omega_m) &= -fG_{12}^{f}(\boldsymbol{k}, \omega_m) \\ &\quad - \mathcal{Z}J_2[\eta + f\mathrm{v}_2]G_{12}^{f}(\boldsymbol{k}, \omega_m) \\ &\quad - 2\mathcal{Z}A_{\boldsymbol{k}}[\eta + f\mathrm{v}_1]G_{22}^{f}(\boldsymbol{k}, \omega_m) \\ &\quad + 2\mathcal{Z}B_{\boldsymbol{k}}[\eta + f\mathrm{v}_1]G_{22}^{f-}(\boldsymbol{k}, \omega_m), \quad (63) \end{aligned}$$

where, as before, $\mathcal{Z}$ is the coordination number, and we introduce

$$A_{\boldsymbol{k}} = A\gamma_{\boldsymbol{k}}, \quad B_{\boldsymbol{k}} = (\Re B)\gamma_{\boldsymbol{k}}' + (\Im B)\gamma_{\boldsymbol{k}}, \quad (64)$$

$$\gamma_{\boldsymbol{k}} = \frac{1}{2}(\cos k_x + \cos k_y), \quad \gamma_{\boldsymbol{k}}' = \frac{1}{2}(\cos k_x - \cos k_y).$$

From these we can write down the following two equations:

$$\begin{aligned} \frac{i\omega_m}{2\mathcal{Z}\eta}G_{12} &= \frac{J_2}{2}G_{12} + A_{\boldsymbol{k}}G_{22} - B_{\boldsymbol{k}}G_{22}^{-}, \quad (65) \\ \frac{i\omega_m}{2\mathcal{Z}\eta}G_{12}^{(1)} &= \frac{1}{2\mathcal{Z}\eta}G_{12} \\ &\quad + \frac{\mathrm{v}_2}{\eta}\frac{J_2}{2}G_{12} + \frac{J_2}{2}G_{12}^{(1)} + \frac{\mathrm{v}_1}{\eta}A_{\boldsymbol{k}}G_{22} + A_{\boldsymbol{k}}G_{22}^{(1)} \\ &\quad - \frac{\mathrm{v}_1}{\eta}B_{\boldsymbol{k}}G_{22}^{-} - B_{\boldsymbol{k}}G_{22}^{(1)-}, \quad (66) \end{aligned}$$

where in all equations we drop the wave vector and frequency dependencies for the Green's functions, that is $G = G(\boldsymbol{k}, \omega_m)$ and $G^{(1)} = G^{(1)}(\boldsymbol{k}, \omega_m)$.

In the same way we obtain the equations of motion for the other Green's functions (see Eq. (54)) within the RPA scheme. The final systems of equations for zeroth- and first-order quantities can be written as

$$\left(\frac{i\omega_m}{2\mathcal{Z}\eta} - \frac{J_2}{2}\right)G_{12} = A_{\boldsymbol{k}}G_{22} - B_{\boldsymbol{k}}G_{22}^{-}, \qquad \left(\frac{i\omega_m}{2\mathcal{Z}\eta} + \frac{J_2}{2}\right)G_{12}^{-} = -A_{\boldsymbol{k}}G_{22}^{-} + B_{\boldsymbol{k}}^{*}G_{22},$$

$$\left(\frac{i\omega_m}{2\mathcal{Z}\eta} - \frac{J_2}{2}\right)G_{22} = A_{\boldsymbol{k}}G_{12} - B_{\boldsymbol{k}}G_{12}^{-} - \frac{1}{\mathcal{Z}}, \quad \left(\frac{i\omega_m}{2\mathcal{Z}\eta} + \frac{J_2}{2}\right)G_{22}^{-} = -A_{\boldsymbol{k}}G_{12}^{-} + B_{\boldsymbol{k}}^{*}G_{12};$$

$$(67)$$

$$\left(\frac{i\omega_m}{2\mathcal{Z}\eta} - \frac{J_2}{2}\right)G_{12}^{(1)} = A_{\boldsymbol{k}}G_{22}^{(1)} - B_{\boldsymbol{k}}G_{22}^{(1)-} + \left\{\frac{\mathrm{v}_2}{\eta}\frac{J_2}{2} + \frac{\mathrm{v}_1}{\eta}\left(\frac{i\omega_m}{2\mathcal{Z}\eta} - \frac{J_2}{2}\right) + \frac{1}{2\mathcal{Z}\eta}\right\}G_{12},$$

$$\left(\frac{i\omega_m}{2\mathcal{Z}\eta} - \frac{J_2}{2}\right)G_{22}^{(1)} = A_{\boldsymbol{k}}G_{12}^{(1)} - B_{\boldsymbol{k}}G_{12}^{(1)-} + \left\{\frac{\mathrm{v}_1}{\eta}\frac{J_2}{2} + \frac{\mathrm{v}_2}{\eta}\left(\frac{i\omega_m}{2\mathcal{Z}\eta} - \frac{J_2}{2}\right)\right\}G_{22},$$

$$\left(\frac{i\omega_m}{2\mathcal{Z}\eta} + \frac{J_2}{2}\right)G_{12}^{(1)-} = -A_{\boldsymbol{k}}G_{22}^{(1)-} + B_{\boldsymbol{k}}^{*}G_{22}^{(1)} - \left\{\frac{\mathrm{v}_2}{\eta}\frac{J_2}{2} - \frac{\mathrm{v}_1}{\eta}\left(\frac{i\omega_m}{2\mathcal{Z}\eta} + \frac{J_2}{2}\right) + \frac{1}{2\mathcal{Z}\eta}\right\}G_{12}^{-},$$

$$\left(\frac{i\omega_m}{2\mathcal{Z}\eta} + \frac{J_2}{2}\right)G_{22}^{(1)-} = -A_{\boldsymbol{k}}G_{12}^{(1)-} + B_{\boldsymbol{k}}^{*}G_{12}^{(1)} - \left\{\frac{\mathrm{v}_1}{\eta}\frac{J_2}{2} - \frac{\mathrm{v}_2}{\eta}\left(\frac{i\omega_m}{2\mathcal{Z}\eta} + \frac{J_2}{2}\right)\right\}G_{22}^{-};$$

$$(68)$$

$$\left(\frac{\mathrm{i}\omega_m}{2\mathcal{Z}\eta} - \frac{J_2}{2}\right)G_{21}^{(1)} = A_{\boldsymbol{k}}G_{11}^{(1)} - B_{\boldsymbol{k}}G_{11}^{(1)-} + \left\{\frac{\mathrm{v}_1}{\eta}\frac{J_2}{2} + \frac{\mathrm{v}_2}{\eta}\left(\frac{\mathrm{i}\omega_m}{2\mathcal{Z}\eta} - \frac{J_2}{2}\right)\right\}G_{12},$$

$$\left(\frac{\mathrm{i}\omega_m}{2\mathcal{Z}\eta} - \frac{J_2}{2}\right)G_{11}^{(1)} = A_{\boldsymbol{k}}G_{21}^{(1)} - B_{\boldsymbol{k}}G_{21}^{(1)-} + \left\{\frac{\mathrm{v}_2}{\eta}\frac{J_2}{2} + \frac{\mathrm{v}_1}{\eta}\left(\frac{\mathrm{i}\omega_m}{2\mathcal{Z}\eta} - \frac{J_2}{2}\right) + \frac{1}{2\mathcal{Z}\eta}\right\}G_{22},$$

$$\left(\frac{\mathrm{i}\omega_m}{2\mathcal{Z}\eta} + \frac{J_2}{2}\right)G_{21}^{(1)-} = -A_{\boldsymbol{k}}G_{11}^{(1)-} + B_{\boldsymbol{k}}^*G_{11}^{(1)} - \left\{\frac{\mathrm{v}_1}{\eta}\frac{J_2}{2} - \frac{\mathrm{v}_2}{\eta}\left(\frac{\mathrm{i}\omega_m}{2\mathcal{Z}\eta} + \frac{J_2}{2}\right)\right\}G_{12}^-,$$

$$\left(\frac{\mathrm{i}\omega_m}{2\mathcal{Z}\eta} + \frac{J_2}{2}\right)G_{11}^{(1)-} = -A_{\boldsymbol{k}}G_{21}^{(1)-} + B_{\boldsymbol{k}}^*G_{21}^{(1)} - \left\{\frac{\mathrm{v}_2}{\eta}\frac{J_2}{2} - \frac{\mathrm{v}_1}{\eta}\left(\frac{\mathrm{i}\omega_m}{2\mathcal{Z}\eta} + \frac{J_2}{2}\right) + \frac{1}{2\mathcal{Z}\eta}\right\}G_{22}^-,$$

$$(69)$$

where we have taken into account the relations

$$G_{12} = G_{21}, \quad G_{11} = G_{22},$$
$$G_{12}^- = G_{21}^-, \quad G_{11}^- = G_{22}^-. \tag{70}$$

The poles of the zero-order Green's functions G have to be the same as the poles found for the first-order ones $G^{(1)}$. This can be seen directly by comparing the structure of the systems of equations for the corresponding quantities: the system in Eq. (67) for the zero-order functions is identical with the systems in Eqs. (68,69) for the first-order ones, except for the free terms. The free terms in the first-order systems are determined by the zero-order Green's functions, thus, the first-order quantities $G^{(1)}$ can be written down in terms of the solution for the zero-order system of Eq. (67), and the as yet unknown quantities v_1 and v_2.

To calculate $\mathrm{v}_{1,2}$ we use a relation connecting v and the Green's functions $G^{(1)}(\boldsymbol{k}, 0^-)$. From the definitions in Eq. (54) and the expansion in Eq. (57) we have

$$G_{ii}^f(0^-) = \frac{1}{2} - \langle\sigma_i^z\rangle^f = \frac{1}{2} - \eta - f\mathrm{v}_i, \tag{71}$$

while the expansion in Eq. (56) leads to

$$G_{ii}^f(0^-) = G_{ii}(0^-) + fG_{ii}^{(1)}(0^-) = \frac{1}{2} - \eta + fG_{ii}^{(1)}(0^-). \tag{72}$$

Thus, we can write down $-\mathrm{v}_i = G_{ii}^{(1)}(0^-)$, and after Fourier summation one obtains

$$-\mathrm{v}_1 = \frac{2}{N}\sum_{\boldsymbol{k}}G_{11}^{(1)}(\boldsymbol{k}, 0^-), \tag{73}$$

$$-\mathrm{v}_2 = \frac{2}{N}\sum_{\boldsymbol{k}}G_{22}^{(1)}(\boldsymbol{k}, 0^-). \tag{74}$$

The solution of the system in Eq. (68) gives us the first-order Green's function $G_{22}^{(1)}(\boldsymbol{k}, \omega_m)$ and therefore v_2. Similarly, to find v_1 we use Eq. (69).

The solution of the system of equations in Eq. (67) for the zeroth-order Green's functions turns out to be

$$G_{12}(\boldsymbol{k}, \omega_n) = -\frac{\eta}{2}\left\{\left(1 + \frac{J_2/2 + A_{\boldsymbol{k}}}{\omega_1(\boldsymbol{k})}\right)\frac{1}{\mathrm{i}\omega_n - \varepsilon_1(\boldsymbol{k})} + \left(1 - \frac{J_2/2 + A_{\boldsymbol{k}}}{\omega_1(\boldsymbol{k})}\right)\frac{1}{\mathrm{i}\omega_n + \varepsilon_1(\boldsymbol{k})}\right.$$
$$\left. - \left(1 + \frac{J_2/2 - A_{\boldsymbol{k}}}{\omega_2(\boldsymbol{k})}\right)\frac{1}{\mathrm{i}\omega_n - \varepsilon_2(\boldsymbol{k})} - \left(1 - \frac{J_2/2 - A_{\boldsymbol{k}}}{\omega_2(\boldsymbol{k})}\right)\frac{1}{\mathrm{i}\omega_n + \varepsilon_2(\boldsymbol{k})}\right\},$$

$$G_{22}(\boldsymbol{k}, \omega_n) = -\frac{\eta}{2}\left\{\left(1 + \frac{J_2/2 + A_{\boldsymbol{k}}}{\omega_1(\boldsymbol{k})}\right)\frac{1}{\mathrm{i}\omega_n - \varepsilon_1(\boldsymbol{k})} + \left(1 - \frac{J_2/2 + A_{\boldsymbol{k}}}{\omega_1(\boldsymbol{k})}\right)\frac{1}{\mathrm{i}\omega_n + \varepsilon_1(\boldsymbol{k})}\right.$$
$$\left. + \left(1 + \frac{J_2/2 - A_{\boldsymbol{k}}}{\omega_2(\boldsymbol{k})}\right)\frac{1}{\mathrm{i}\omega_n - \varepsilon_2(\boldsymbol{k})} + \left(1 - \frac{J_2/2 - A_{\boldsymbol{k}}}{\omega_2(\boldsymbol{k})}\right)\frac{1}{\mathrm{i}\omega_n + \varepsilon_2(\boldsymbol{k})}\right\},$$

$$G_{12}^-(\boldsymbol{k}, \omega_n) = -\frac{\eta}{2}B_{\boldsymbol{k}}^*\left\{\frac{1}{\omega_1(\boldsymbol{k})}\left(\frac{1}{\mathrm{i}\omega_n - \varepsilon_1(\boldsymbol{k})} - \frac{1}{\mathrm{i}\omega_n + \varepsilon_1(\boldsymbol{k})}\right) + \frac{1}{\omega_2(\boldsymbol{k})}\left(\frac{1}{\mathrm{i}\omega_n - \varepsilon_2(\boldsymbol{k})} - \frac{1}{\mathrm{i}\omega_n + \varepsilon_2(\boldsymbol{k})}\right)\right\},$$

$$G_{22}^-(\boldsymbol{k}, \omega_n) = -\frac{\eta}{2}B_{\boldsymbol{k}}^*\left\{\frac{1}{\omega_1(\boldsymbol{k})}\left(\frac{1}{\mathrm{i}\omega_n - \varepsilon_1(\boldsymbol{k})} - \frac{1}{\mathrm{i}\omega_n + \varepsilon_1(\boldsymbol{k})}\right) - \frac{1}{\omega_2(\boldsymbol{k})}\left(\frac{1}{\mathrm{i}\omega_n - \varepsilon_2(\boldsymbol{k})} - \frac{1}{\mathrm{i}\omega_n + \varepsilon_2(\boldsymbol{k})}\right)\right\},$$

$$(75)$$

where the spectra for the out-of-plane $\varepsilon_1(\boldsymbol{k})$ and in-plane $\varepsilon_2(\boldsymbol{k})$ modes[14] are given by

$$
\begin{aligned}
\varepsilon_1(\boldsymbol{k}) &= 2\mathcal{Z}\eta\omega_1(\boldsymbol{k}) = 2\mathcal{Z}\eta\sqrt{(J_2/2 + A_{\boldsymbol{k}})^2 - |B_{\boldsymbol{k}}|^2}, \\
\varepsilon_2(\boldsymbol{k}) &= 2\mathcal{Z}\eta\omega_2(\boldsymbol{k}) = 2\mathcal{Z}\eta\sqrt{(J_2/2 - A_{\boldsymbol{k}})^2 - |B_{\boldsymbol{k}}|^2}.
\end{aligned}
\tag{76}
$$

After the substitution of the results in Eq. (75) into the system of equations in Eqs. (68,69), and then using the solutions for $G_{11}^{(1)}(\boldsymbol{k}, \omega_m)$, $G_{22}^{(1)}(\boldsymbol{k}, \omega_m)$, the results for quantities v_1 and v_2 are found to be

$$
\begin{aligned}
v_1 - v_2 &= \frac{\eta^2 C_1}{1 + 4\eta^2 J_2 C_1}, &(77) \\
v_1 + v_2 &= \frac{\eta^2 C_2}{1 - 8\eta^2 C_3}, &(78)
\end{aligned}
$$

where

$$
\begin{aligned}
C_1 &= \frac{2}{N}\sum_{\boldsymbol{k}} 2\left\{\left(1 + \frac{(J_2/2)^2 - A_{\boldsymbol{k}}^2 - |B_{\boldsymbol{k}}|^2}{\omega_1(\boldsymbol{k})\omega_2(\boldsymbol{k})}\right)\frac{n(\varepsilon_1) - n(\varepsilon_2)}{\varepsilon_2(\boldsymbol{k}) - \varepsilon_1(\boldsymbol{k})} - \left(1 - \frac{(J_2/2)^2 - A_{\boldsymbol{k}}^2 - |B_{\boldsymbol{k}}|^2}{\omega_1(\boldsymbol{k})\omega_2(\boldsymbol{k})}\right)\frac{n(\varepsilon_1) + n(\varepsilon_2) + 1}{\varepsilon_1(\boldsymbol{k}) + \varepsilon_2(\boldsymbol{k})}\right\}, \\
C_2 &= \frac{2}{N}\sum_{\boldsymbol{k}} \left\{\frac{(J_2/2 + A_{\boldsymbol{k}})^2\beta/2}{\omega_1^2(\boldsymbol{k})\sinh^2\frac{\beta\varepsilon_1}{2}} + \frac{|B_{\boldsymbol{k}}|^2[2n(\varepsilon_1) + 1]}{\omega_1^2(\boldsymbol{k})\varepsilon_1(\boldsymbol{k})} + \frac{(J_2/2 - A_{\boldsymbol{k}})^2\beta/2}{\omega_2^2(\boldsymbol{k})\sinh^2\frac{\beta\varepsilon_2}{2}} + \frac{|B_{\boldsymbol{k}}|^2[2n(\varepsilon_2) + 1]}{\omega_2^2(\boldsymbol{k})\varepsilon_2(\boldsymbol{k})}\right\}, \\
C_3 &= \frac{2}{N}\sum_{\boldsymbol{k}} \left\{\frac{(J_2/2 + A_{\boldsymbol{k}})\beta/2}{\sinh^2\frac{\beta\varepsilon_1}{2}} + \frac{(J_2/2 - A_{\boldsymbol{k}})\beta/2}{\sinh^2\frac{\beta\varepsilon_2}{2}}\right\}, \quad \text{here } n(\varepsilon_{1,2}) = [\exp(\beta\varepsilon_{1,2}(\boldsymbol{k})) - 1]^{-1}.
\end{aligned}
\tag{79}
$$

Now let us find the quantities which determine a linear response to a magnetic field applied to the one of sublattice – see Eqs. (25,26). The longitudinal z components of the susceptibility in the characteristic representation are given by

$$
\chi_{11}^{\sigma^z\sigma^z} = \left.\frac{\partial\langle\sigma_1^z\rangle^f}{\partial f}\right|_{f=0} = v_1, \quad \chi_{12}^{\sigma^z\sigma^z} = \left.\frac{\partial\langle\sigma_2^z\rangle^f}{\partial f}\right|_{f=0} = v_2,
\tag{80}
$$

where the expansion of Eq. (57) was used. The transverse x and y components of the susceptibility tensor are determined in the terms of Green's functions as

$$
\begin{aligned}
\chi_{11}^{\sigma^\alpha\sigma^{\alpha'}} &= \frac{2}{N}\sum_{i,i'}\int_0^\beta \langle T_\tau\sigma_i^\alpha(\tau)\sigma_{i'}^{\alpha'}(0)\rangle\mathrm{d}\tau, \\
\chi_{12}^{\sigma^\alpha\sigma^{\alpha'}} &= \frac{2}{N}\sum_{i,j}\int_0^\beta \langle T_\tau\sigma_i^\alpha(\tau)\sigma_j^{\alpha'}(0)\rangle\mathrm{d}\tau,
\end{aligned}
\tag{81}
$$

where $\alpha = x, y$. By substituting the solutions in Eq. (75) into the definition in Eq. (81) for the transverse components of susceptibility, we easily obtain *exactly the same result* that we have already found within our MFA calculations – that is, Eq. (43).

Then, using Eqs. (27)-(29) the components of the susceptibility in the initial coordinate system of Eq. (1) are

found to be

$$
\begin{aligned}
\chi^x &= \frac{1}{4}\frac{1}{J_1 + J_2}, &(82) \\
\chi^y &= \frac{1}{4}\frac{\sin^2(\theta)}{J_2 - J_3} + \cos^2(\theta)[v_1 - v_2], &(83) \\
\chi^z &= \frac{1}{4}\frac{\cos^2(\theta)}{J_2 + J_3} + \sin^2(\theta)[v_1 + v_2]. &(84)
\end{aligned}
$$

For completeness, we mention that we have also performed the theoretical investigation of this model (1) within spin-wave (SW) theory, and the final result for the components of static susceptibility turns out to be

$$
\begin{aligned}
\chi^{x\ SW} &= \frac{1}{4}\frac{1}{J_1 + J_2}, &(85) \\
\chi^{y\ SW} &= \frac{1}{4}\frac{\sin^2(\theta)}{J_2 - J_3} + \cos^2(\theta)S^2 C_1\big|_{\eta\to S}, &(86) \\
\chi^{z\ SW} &= \frac{1}{4}\frac{\cos^2(\theta)}{J_2 + J_3} + \sin^2(\theta)S^2 C_2\big|_{\eta\to S}. &(87)
\end{aligned}
$$

It can be noted that the difference in the results within the RPA, Eqs. (82)-(84), and spin-wave theory, Eqs. (85)-(87), came from the calculation of the components of the susceptibility in the direction of the sublattice magnetization (that is $\chi_{11}^{\sigma^z\sigma^z}$ and $\chi_{12}^{\sigma^z\sigma^z}$). The spin-wave theory gives unity in the denominator of the expressions for $\chi_{11}^{\sigma^z\sigma^z}$ and $\chi_{12}^{\sigma^z\sigma^z}$ in Eq. (77), and $S = 1/2$ instead of the order parameter η everywhere in the numerator.

The similar situation takes place for antiferromagnetic Heisenberg model within the RPA scheme[17] and spin-wave theory.[31]

We also mention that the transverse components of the susceptibility in the characteristic representation (43) are equal within the MFA, RPA, and SW theories.

B. Related Thermodynamic quantities

In order for the above RPA theory to be complete, we need to determine the behaviour of the order parameter and the transition temperature.

The above expressions for the components of susceptibility Eqs. (83,84), and for the elementary excitations (spin waves) given by Eq. (76), include the as-yet-unknown value of the order parameter η. From the definition on the Green's functions we can obtain

$$G_{nn}(\tau = 0^-) = \langle \sigma_n^- \sigma_n^+ \rangle = \frac{1}{2} - \eta, \quad (88)$$

where $\quad G_{nn}(0^-) = \frac{2}{N} \sum_{\boldsymbol{k}} G_{22}(\boldsymbol{k}, 0^-).$

Substituting $G_{22}(\boldsymbol{k}, \omega)$ from Eq. (75), and performing the summation on the Matsubara frequencies, the equation on the order parameter turns out to be

$$\frac{1}{\eta} = \frac{2}{N} \sum_{\boldsymbol{k}} \left\{ \frac{J_2/2 + A_{\boldsymbol{k}}}{\omega_1(\boldsymbol{k})} [2n(\varepsilon_1) + 1] \right.$$
$$\left. + \frac{J_2/2 - A_{\boldsymbol{k}}}{\omega_2(\boldsymbol{k})} [2n(\varepsilon_2) + 1] \right\}. \quad (89)$$

Since order parameter (89) (sublattice magnetization) is temperature dependent, it follows that the spectrum of elementary excitations (Eq. (76)) is also temperature dependent.

The Néel temperature at which η vanishes within the adopted RPA approximation is determined by

$$T_{\mathrm{N}} = \left\{ \frac{1}{4} \frac{2}{N} \sum_{\boldsymbol{k}} \left(\frac{J_2/2 + A_{\boldsymbol{k}}}{\omega_1^2(\boldsymbol{k})} + \frac{J_2/2 - A_{\boldsymbol{k}}}{\omega_2^2(\boldsymbol{k})} \right) \right\}^{-1}. \quad (90)$$

By putting $\eta \to 0$ we can find that z-component of susceptibility χ^z in Eq. (84)

$$\chi^z \Big|_{\eta \to 0} = \frac{1}{4} \frac{\cos^2(\theta)}{J_2 + J_3} + \sin^2(\theta) \frac{T C_2 |_{\eta \to 0}}{1 - T T_{\mathrm{N}}}, \quad (91)$$

diverges at the Néel temperature, whereas other components of susceptibility remain finite as the Néel point is approached from below.

C. Susceptibility in the paramagnetic case

When the temperature of the system is above the Néel temperature, T_N, there still exists short-range magnetic order. To model such an order[17] we introduce a fictitious field h pointing in the direction of the sublattice magnetization, that is the z direction in the characteristic representation. To this end, the Hamiltonian

$$H_h = H_{\mathrm{CR}} - h \sum_i \sigma_i^z - h \sum_j \sigma_j^z \quad (92)$$

is used, and the limit $h \to 0$ is taken after the calculation is carried out. To obtain the susceptibility above the Néel temperature, it is convenient to introduce an order parameter defined by

$$y = \lim_{h \to 0} (2\mathcal{Z}\eta/h). \quad (93)$$

The calculations for the model are very similar to the ones above presented. It is easy to show that paramagnetic version of the equation on the order parameter in Eq. (89) leads to

$$\frac{1}{y} = \frac{2}{N} \sum_{\boldsymbol{k}} \frac{1}{\mathcal{Z}\beta} \left\{ \frac{1 + y(J_2/2 + A_{\boldsymbol{k}})}{(1 + y(J_2/2 + A_{\boldsymbol{k}}))^2 - y^2 |B_{\boldsymbol{k}}|^2} \right.$$
$$\left. + \frac{1 + y(J_2/2 - A_{\boldsymbol{k}})}{(1 + y(J_2/2 - A_{\boldsymbol{k}}))^2 - y^2 |B_{\boldsymbol{k}}|^2} \right\}. \quad (94)$$

The quantity y approaches to infinity as the temperature is lowered to T_{N}. Indeed, putting $y \to \infty$ in Eq. (94) we find the temperature at which y diverges, which is nothing but Néel temperature.

By a procedure similar to the above presented (that is, the RPA scheme below T_N) the different components of the magnetic susceptibility in the paramagnetic phase are found to be

$$\chi^x = \frac{1}{4} \frac{1}{J_1 + J_2 + 2/y}, \quad (95)$$

$$\chi^y = \frac{1}{4} \frac{\sin^2(\theta)}{J_2 - J_3 + 2/y} + \cos^2(\theta) \frac{y^2 D_1}{1 + 8y(1 + yJ_2/2)D_1}, \quad (96)$$

$$\chi^z = \frac{1}{4} \frac{\cos^2(\theta)}{J_2 + J_3 + 2/y} + \sin^2(\theta) \frac{y^2 D_2}{1 - 8y^2 D_3}, \quad (97)$$

where

$$D_1 = \frac{1}{2\mathcal{Z}^2\beta}\frac{2}{N}\sum_{\boldsymbol{k}}2\frac{(1+y(J_2/2+A_{\boldsymbol{k}}))(1+y(J_2/2-A_{\boldsymbol{k}})) - y^2|B_{\boldsymbol{k}}|^2}{\{(1+y(J_2/2+A_{\boldsymbol{k}}))^2 - y^2|B_{\boldsymbol{k}}|^2\}\{(1+y(J_2/2-A_{\boldsymbol{k}}))^2 - y^2|B_{\boldsymbol{k}}|^2\}},$$

$$D_2 = \frac{1}{2\mathcal{Z}^2\beta}\frac{2}{N}\sum_{\boldsymbol{k}}\left[\frac{(1+y(J_2/2+A_{\boldsymbol{k}}))^2 + y^2|B_{\boldsymbol{k}}|^2}{\{(1+y(J_2/2+A_{\boldsymbol{k}}))^2 - y^2|B_{\boldsymbol{k}}|^2\}^2} + \frac{(1+y(J_2/2-A_{\boldsymbol{k}}))^2 + y^2|B_{\boldsymbol{k}}|^2}{\{(1+y(J_2/2-A_{\boldsymbol{k}}))^2 - y^2|B_{\boldsymbol{k}}|^2\}^2}\right],$$

$$D_3 = \frac{1}{2\mathcal{Z}^2\beta}\frac{2}{N}\sum_{\boldsymbol{k}}\left[\frac{1+y(J_2/2+A_{\boldsymbol{k}})}{(1+y(J_2/2+A_{\boldsymbol{k}}))^2 - y^2|B_{\boldsymbol{k}}|^2} + \frac{1+y(J_2/2-A_{\boldsymbol{k}})}{(1+y(J_2/2-A_{\boldsymbol{k}}))^2 - y^2|B_{\boldsymbol{k}}|^2}\right].$$

$$(98)$$

By putting $y \to \infty$ we obtain that the components of susceptibility χ^x and χ^y are continuous at the Néel point, whereas the z-component of susceptibility diverges in the $y \to \infty$ limit at the Néel point, the latter result reflecting the presence of the spontaneous canted ferromagnetic moment in the z direction.

D. Susceptibility in the $T = 0$ limit

As we will present in the results discussion, the dimensionality of the parameter space that seems to be relevant to the cuprates is large, but there are only a few important values that determine the physical properties of the system. Here we discuss two key experimentally obtainable quantities, and their relation to the above theory.

It has been reported, using inelastic neutron scattering, that the out-of-plane (ε_1) and in-plane (ε_2) spin-wave gaps are 5.0 and 2.3 meV, respectively, in the LTO phase of La$_2$CuO$_4$ crystal.[5] Using these results let us predict the ratio of the components of susceptibility χ^y/χ^x. The zone-centre ($\boldsymbol{k} = 0$) spin-wave gaps are given by

$$\begin{aligned}\varepsilon_1 &= \mathcal{Z}\eta\sqrt{(J_2 + J_1)(J_2 - J_3)}, \\ \varepsilon_2 &= \mathcal{Z}\eta\sqrt{(J_2 - J_1)(J_2 + J_3)},\end{aligned} \quad (99)$$

and they are real if $J_2 < J_1, J_3$. So, from these relations we obtain

$$\varepsilon_2 < \varepsilon_1 \quad \Leftrightarrow \quad J_1 > J_3. \quad (100)$$

Also, in the $T = 0$ limit the y component of the susceptibility in Eq. (46) is given by

$$\chi^{y\ MFA} = \frac{1}{4}\frac{\sin^2(\theta)}{J_2 - J_3} = \frac{1}{4}\frac{J_2 - J_1}{J_2^2 - J_3^2},$$

$$\text{then} \quad \frac{\chi^{y\ MFA}}{\chi^{x\ MFA}} = \frac{J_2^2 - J_1^2}{J_2^2 - J_3^2}. \quad (101)$$

Therefore, within the MFA

$$\chi^{x\ MFA} > \chi^{y\ MFA} \quad \Leftrightarrow \quad J_1 > J_3. \quad (102)$$

Thus, if $\varepsilon_2 < \varepsilon_1$ ($\varepsilon_2 > \varepsilon_1$), in the limit of zero temperature the MFA predicts that $\chi^y < \chi^x$ ($\chi^y > \chi^x$).

In the limit of the small anisotropy $d, \Gamma \ll J$ the components of the susceptibility at $T = 0$ within the MFA turn out to be

$$\chi^{x\ MFA} \approx \chi^{z\ MFA} \approx \frac{1}{8J},$$

$$\chi^{y\ MFA} \approx \frac{d^2}{32J^2(\Gamma_1 - \Gamma_3)}, \quad (103)$$

while the expressions for the spin-wave gaps are

$$\varepsilon_1 \approx \mathcal{Z}\eta\sqrt{2J(\Gamma_1 - \Gamma_3)}, \ \varepsilon_2 \approx \mathcal{Z}\eta d/\sqrt{2}. \quad (104)$$

We can see that components $\chi^{x,z}$ are almost independent of the anisotropy parameters, while the χ^y component is very sensitive to the *ratio* between the anti-symmetric d and symmetric $\Gamma_1 - \Gamma_3$ parameters of anisotropy. Then, the ratio between the components of the susceptibility is given by

$$\frac{\chi^{x,z\ MFA}}{\chi^{y\ MFA}} \approx \left(\frac{\varepsilon_1}{\varepsilon_2}\right)^2. \quad (105)$$

It can be noted that within the MFA scheme the different components of the susceptibility, i.e. χ^x, χ^y and χ^z, are determined by the contributions from the *transverse components* of the susceptibility in the characteristic representation. Indeed, as should be expected, the longitudinal components of the susceptibility in the CR (see Eq. (38)) are equal to zero in the $T = 0$ limit. As showed earlier in this paper, in the characteristic representation the RPA and SW theories lead to the same result for the transverse components of the susceptibility as the MFA does. Since the longitudinal components in the CR, given by the Eq. (77) within the RPA, and their simplified expressions within the SW theory (see Eqs. (86,87)) become negligibly small in the $T = 0$ limit, we predict that RPA, SW and MFA within the reasonable range of the model parameters ($d, \Gamma \ll J$) satisfy the ratio of Eq. (105), and the different components of the susceptibility at $T = 0$ can be approximated by the Eq. (103).

We also note the analogy with the pure 3D Heisenberg model where, in the limit of zero temperature, all approximations considered here give the same magnitude

for the transverse components of the susceptibility, and zero for the longitudinal one.[17]

V. RESULTS OF CALCULATIONS

In this section we present the results of a numerical investigation of the magnetic properties of the system modelled by the Hamiltonian given by Eq. (1) based on the above presented analytical formulae. Specifically, we are interested in the temperature dependencies of the various components of the susceptibility for different values (specifically, ratios) of the model parameters. Further, we will numerically demonstrate the correlation between the magnitudes of the two spin-wave gaps in the excitation spectrum and the behaviour of the susceptibility components; this relation was discussed analytically in the previous subsection. Also, and most importantly, we will make clear the role played by quantum fluctuations by comparing the results of the different approximation schemes.

In what follows, we will mainly examine one set of parameters that are suggested from experimental measurements discussed in the previous subsection, and this will allow us to "zero in" on a parameter regime. However, since have developed the theory for one plane and not a 3d solid, we do not necessarily expect this set of parameters to be representative of a system like La_2CuO_4; instead, as we discussed in the introduction to this paper, this approach will allow us to determine if a one-plane approach is adequate, since, as we and others have discussed, a true $T_c > 0$ phase transition is possible for one plane and thus could possibly be sufficient for this system.

In the present calculations we express all model parameters in terms of J. Also, as will be made clear below, instead of using the set of parameters Γ_1, Γ_2, and Γ_3, we deal with combination of parameters $\Gamma_1 - \Gamma_3$, $\Gamma_1 + \Gamma_3$, and Γ_2. The chosen magnitudes of the model parameters d and $\overleftrightarrow{\Gamma}$ give the reported magnitude of gaps in the spectrum[5,32]

$$\varepsilon_o = \varepsilon_1 \approx 5 \text{ meV}, \qquad \varepsilon_i = \varepsilon_2 \approx 2.3 \text{ meV}, \qquad (106)$$

at the temperature $T = T_N/3$ for the superexchange value $J = 130$ meV.[5] This leads to the parameters given by

$$d/J = 0.02, \qquad (\Gamma_1 - \Gamma_3)/J = 0.42 \times 10^{-3}, \quad (107)$$

where, as discussed below, we have set

$$(\Gamma_1 + \Gamma_3)/J = 0, \qquad \Gamma_2 = 0. \qquad (108)$$

A. The AFM order parameter, spin-wave excitations, and T_N

To examine the different analytical schemes used in the previous sections, we compare the representative solutions of the order parameter, η, within the RPA method,

Eq. (89), and within the MFA, Eq. (32). Most interestingly, we note the results shown in Fig. 3(a) look very similar to the corresponding ones for the pure 3D quantum Heisenberg antiferromagnet within the RPA and MFA schemes.[16]

Since the order parameter η is temperature dependent, it follows that within the RPA scheme the spin-wave spectrum (see Eq. (76)) is also temperature dependent. In Fig. 3(b) we present the behaviour of both modes in the excitation spectrum at the long wavelength limit ($\boldsymbol{k} = 0$) (energy gaps) with respect to the relative temperature (T/T_N); these results compare favourably with the experimental measurements of the same quantity.[5]
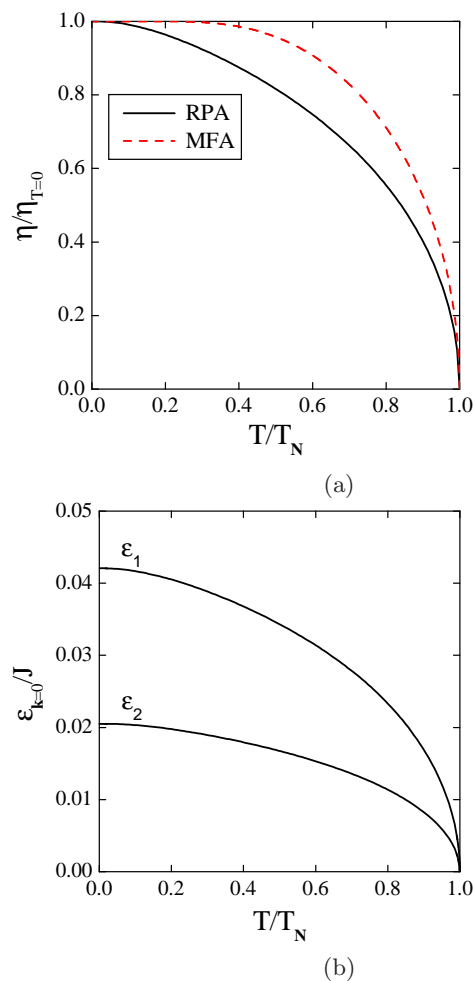

(a)

(b)

FIG. 3: (Color online) The (a) order parameter *vs.* T/T_N within the RPA method (black solid line) and the MFA (red dashed line), and the (b) spin-wave gaps, in units of J, in the spectrum of elementary excitations *vs.* T/T_N within the RPA method. In both of these figures we have used $d/J = 0.02$, $(\Gamma_1 - \Gamma_3)/J = 0.42 \times 10^{-3}$, $\Gamma_1 + \Gamma_3 = 0$, and $\Gamma_2 = 0$.

Now let us show that in contrast to the MFA approach, where $T_N = J_2 \approx J$ is almost independent of the anisotropy, the Néel temperature within the RPA analytical scheme is very sensitive to model parameters d and $\Gamma_1 - \Gamma_3$. Figure 4 shows the zero-temperature en-
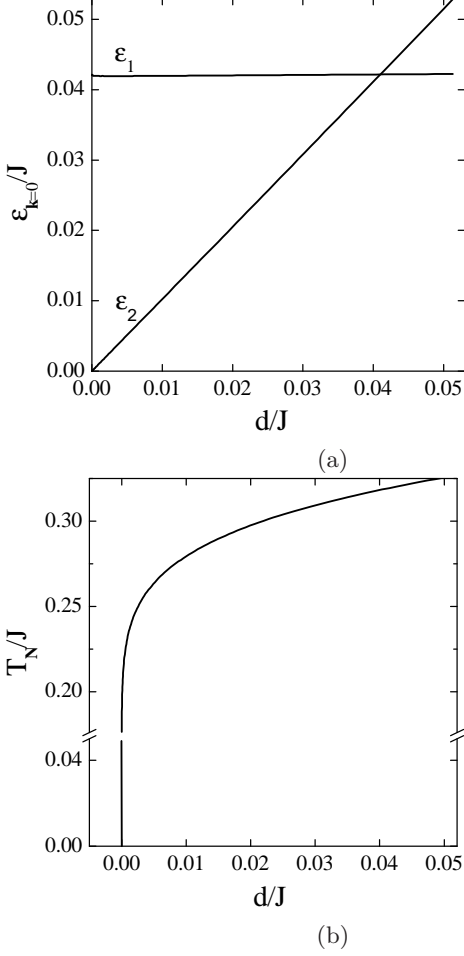
(a)

(b)

FIG. 4: The (a) $T = 0$ energy gaps, in units of J, *vs.* the DM parameter d/J, as well as (b) the Néel temperature T_N, in units of J, *vs* d/J. In both of these figures, $(\Gamma_1 - \Gamma_3)/J = 0.42 \times 10^{-3}$, $\Gamma_1 + \Gamma_3 = 0$, and $\Gamma_2 = 0$.

(a)

(b)

FIG. 5: The (a) energy gaps, in units of J, *vs.* $(\Gamma_1 - \Gamma_3)/J$, and (b) the Néel temperature, in units of J, as function of $(\Gamma_1 - \Gamma_3)/J$.

ergy gaps and the Néel temperature as functions of the DM antisymmetric exchange interaction d/J within the RPA method. As one can see, the energy gap ε_1 is almost independent of the d/J, while ε_2 depends almost linearly on the DM interaction d/J, and in fact goes to the zero in the limit $d/J \to 0$. As a result, when $d/J = 0$ the Goldstone mode appears in the spin-wave spectrum and thermal fluctuations destroy the long-range ordering for any $T > 0$. Consequently, the Néel temperature drops to zero in case of $d = 0$.

In the next two figures we present the dependencies on the model parameter $(\Gamma_1 - \Gamma_3)/J$. Now, the energy gap ε_2 is independent of the parameters of symmetric anisotropy $\overleftrightarrow{\Gamma}$ and thus determined by the DM interaction d/J alone, while the gap ε_1 varies strongly with $(\Gamma_1 - \Gamma_3)/J$. As in the above case, in the limit of $\Gamma_1 - \Gamma_3 \to 0$ the mode ε_2 in the spectrum becomes gapless and, therefore, the transition temperature to the long-range ordered state would be suppressed to zero.
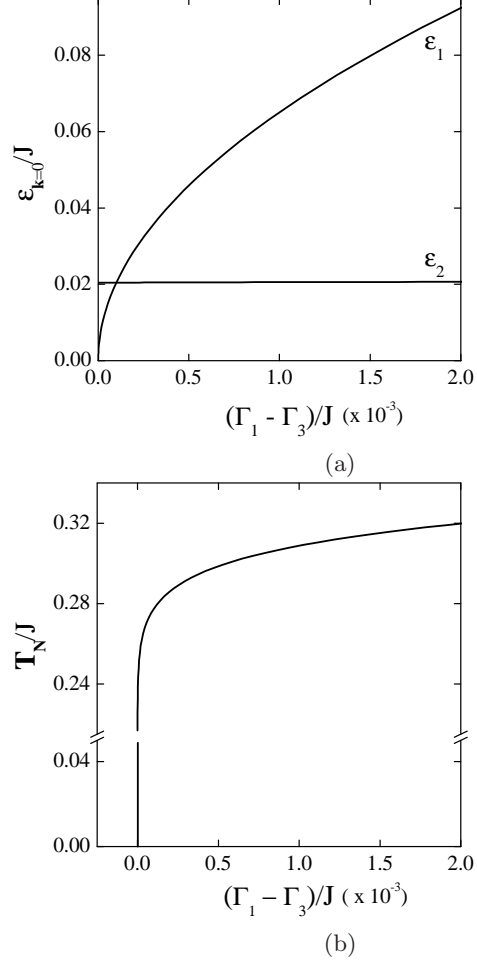
One can understand the above results for the zone-

centre excitation spectrum immediately from the the expressions Eq. (104) in the limit of small anisotropy. Our numerical results, shown in the previous figures, demonstrate that these expressions are valid over a large range of parameter values.

B. Parameters regimes

We now summarize our numerical results with regards to the dependence of various thermodynamic quantities on the material parameters appearing in the Hamiltonian.

Firstly, we find that the Néel temperature is almost independent of the $(\Gamma_1 + \Gamma_3)/J$ within the reasonable range of the model parameters (see below). In fact, in order to argue for the independence of the thermodynamic quantities central to this study on certain material parameters that appear in the Hamiltonian, *viz.* Γ_2 and $\Gamma_1 + \Gamma_3$, in Fig. 6 we show two representative plots for the order parameter and the susceptibility within the RPA scheme
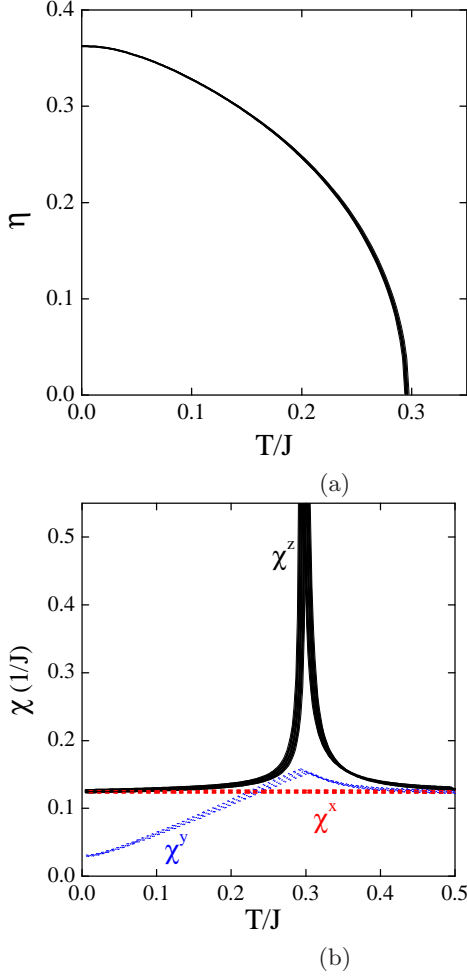
(a)

(b)

FIG. 6: (Color online) The (a) order parameter *vs.* T/J for the different values of Γ_2/J and $(\Gamma_1 + \Gamma_3)/J$, and (b) the susceptibility, in units of $1/J$, *vs.* T/J for the different values of Γ_2 and $\Gamma_1 + \Gamma_3$ discussed in the test. In these plots we have fixed $d/J = 0.02$, and $\Delta\Gamma/J \equiv (\Gamma_1 - \Gamma_3)/J = 0.42 \times 10^{-3}$).

for the constant values of the d and $\Delta\Gamma = \Gamma_1 - \Gamma_3$ (again in units of J). That is, in each of the plots in Fig. 6 we have simultaneously plotted ten data sets each with the different values of the Γ_2 and $\Gamma_1 + \Gamma_3$, where the parameter ratio Γ_2 has been varied from the value $-10^3 \times \Delta\Gamma$ up to the $10^3 \times \Delta\Gamma$, and $\Gamma_1 + \Gamma_3$ from the value $-10^2 \times \Delta\Gamma$ to the $10^2 \times \Delta\Gamma$ (all in units of J). As one can see, even for such a large range of the parameters, one can hardly see the difference of the absolute values of the Néel temperature, order parameter and susceptibility.

Thus, to study the magnetic properties of the system we can use only the DM interaction d and the combination $\Gamma_1 - \Gamma_3$ of the symmetric tensor components as two independent parameters, and so we conclude (similar to others[32,33]) that the system can be studied using $\Gamma_2 = 0$ and $\Gamma_1 + \Gamma_3 = 0$.

In various limits, it can be shown that this result follows from the above presented analytical work. The non-diagonal term Γ_2 of the symmetry anisotropy tensor is

involved in all expression through the combination in the J_4 (Eq. (8)). For the reasonable anisotropy parameters (that is $\Gamma < d \ll J$) the spins are canted by a very small angle $\theta \sim d/J$, and as a result we can neglect the term $\Gamma_2 \sin\theta \sim d\Gamma_2/J$ with respect to d, and hence we can ignore the quantity Γ_2 in all our formulae. Similarly, $\Gamma_1 + \Gamma_3$ is involved in the formulae through the combination in the J_2, J_3, and canted angle θ, where it appeared only as the combination $J + \frac{1}{2}(\Gamma_1 + \Gamma_3)$. Thus, the parameter $\Gamma_1 + \Gamma_3$ can be ignored with respect to the superexchange interaction J (see Eq. (8)).

Therefore, one can assert that the model Hamiltonian of Eq. (1) leads to the same results as, for instance, the model described by the spin Hamiltonian

$$H = \sum_{\langle i,j \rangle} [J\mathbf{S}_i \cdot \mathbf{S}_j - \Delta\Gamma S_i^z S_j^z + \mathbf{D}_{ij}(\mathbf{S}_i \times \mathbf{S}_j)], \quad (109)$$

where we define $\Delta\Gamma \equiv \Gamma_1 - \Gamma_3$.

C. Susceptibility

Now let us consider the main focus of our paper, that being the behaviour of the different components of static uniform magnetic susceptibility as a function of temperature. Our results for χ^x, for the parameters discussed in the previous subsections, are shown in Fig. 7 (recall our earlier result that the MFA and SW theories predict the same T-independent value for this quantity). The x component of susceptibility below the Néel temperature is the temperature independent and is equal to $\approx 1/(8J)$ within the MFA (Eq. (45)), the RPA scheme (Eq. (82)), or spin-wave theory (Eq. (85)). However, above the ordering temperature, the RPA and MFA yield different results, with a weak T-dependence within the RPA, while a strong Curie-like falloff is found within the MFA.
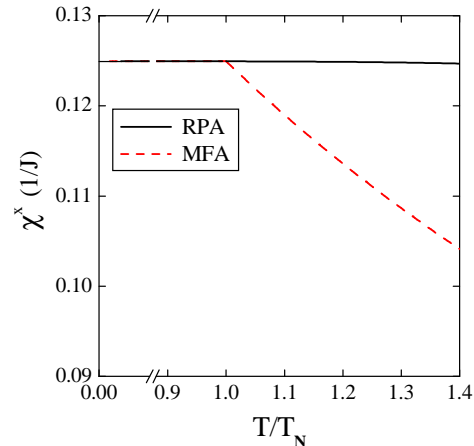

FIG. 7: (Color online) The susceptibility χ^x, in units of $1/J$, within the RPA (black solid line) and MFA (red dashed line), for the parameters values $d/J = 0.02$ and $\Delta\Gamma/J = 0.42 \times 10^{-3}$. Below T_N these theories both predict the same constant value that is independent of temperature.

As we will discuss in a future publication, this behaviour changes if one includes 4-spin ring exchange, or goes beyond the Tyablikov RPA decoupling scheme that we employ in this paper. This is important since the experimental data of Lavrov *et al.*,[6] shows a small nonzero slope of χ^x *vs.* T. Indeed, a successful comparison with the small slope seen below T_N in experimental data[6] necessarily requires that we go beyond the treatment of spin-wave interactions and/or Hamiltonian that are included in this paper. We emphasize that the necessity of going beyond the Tyablikov RPA decoupling to obtain this slope is a manifestation of the presence of strong quantum fluctuations, a theme that will be repeated in our discussion in this and the next section of this paper.

Our results for the y component of the susceptibility, χ^y, are shown in Fig. 8. These plots show that be-

(a)

(b)
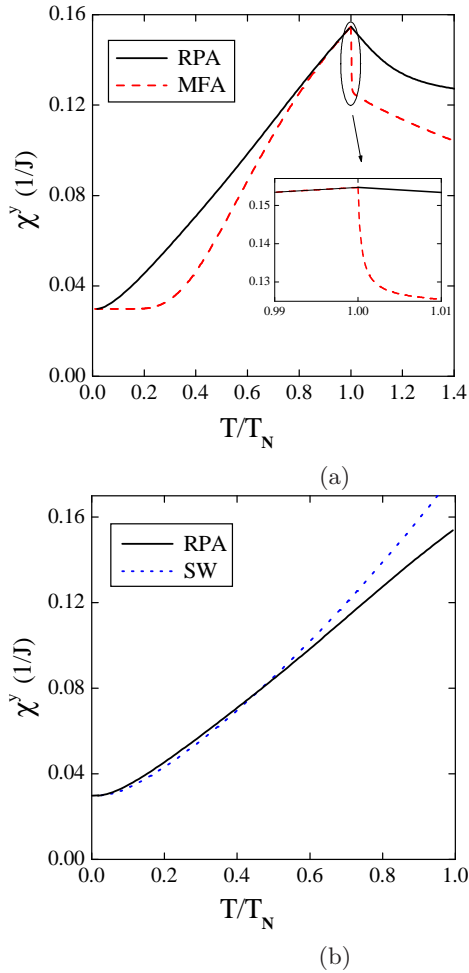
FIG. 8: (Color online) The (a) susceptibility χ^y within the RPA (black solid line) and MFA (red dashed line), and (b) a comparison of the RPA (black solid line) and spin-wave (SW) (blue dotted line) results below T_N. As in previous figures, we are using $d/J = 0.02$ and $\Delta\Gamma/J = 0.42 \times 10^{-3}$.

low the ordering temperature the RPA scheme leads to the good agreement with the MFA scheme near the T_N ($0.8T_N < T < T_N$), and good agreement with the SW

theory at low-T (that is, for $T < T_N/2$). Above the Néel temperature, the RPA and MFA theories lead to very different results. The MFA method gives an abrupt decrease of χ^y to a value that is close to that of the purely transverse component $\chi^x \approx 1/(8J)$ (see inset of this figure), while the RPA leads to a much more gradual decrease of the value of χ^y with the temperature.

The z component of the susceptibility, χ^z, is shown in Fig. 9. We find that at low T, as was also found for χ^y,
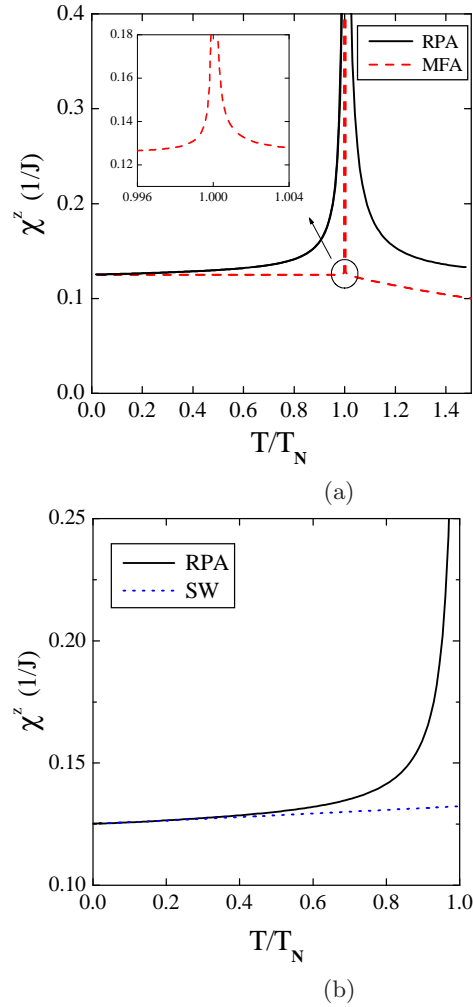

(a)

(b)

FIG. 9: (Color online) The susceptibility χ^z within (a) the RPA (black solid line) and MFA (red dashed line), as well as (b) a comparison of χ^z below the ordering temperature within the RPA (black solid line) and spin-wave (SW) (blue dotted line) theory. As in previous plots, we have used $d/J = 0.02$ and $\Delta\Gamma/J = 0.42 \times 10^{-3}$.

the RPA is in the the good agreement with spin-wave predictions. Near the transition temperature, the RPA method leads to the qualitatively different behaviour of the z component of susceptibility with respect to both the MFA and spin-wave formalisms.

The differences between the MFA *vs.* RPA data shown above can be understood using the following reasoning. Firstly, consider below the Néel temperature. The canted

moments which develop are confined to lie in the $y - z$ plane; as well, they are ferromagnetically ordered in the z-direction (recall that we are studying a single CuO$_2$ plane). Then, one can see that within the MFA the weak FM produces a divergence of the z-component of the susceptibility only in a very narrow temperature region close to the Néel point. Since the MFA does not account for near-neighbour correlations between the spins, away from the immediate vicinity of T_N the weak FM is ignored and χ^z behaves like a T-independent transverse susceptibility (that is, transverse to the ordered AF moment). In contrast to this, the z-component of the susceptibility calculated within the RPA has a strong temperature dependence and shows that the effects of the quantum fluctuations are important in a wide region below the Néel temperature. The other component which shows some differences between the MFA and RPA below the transition is χ^y, and for this component it is seen that since the MFA does not include the reduction of the staggered moment (which is in this direction) due to quantum fluctuations at low temperatures, linear spin-wave theory, and not the MFA, agrees with the RPA for low temperatures.

Further, above the Néel temperature the differences can be understood as follows. In a MFA (that is $T_N^{MFA} \approx J$), both components of the susceptibility χ^y and χ^z are rapidly changing functions in the immediate vicinity of T_N ($\delta T/T_N \sim 0.005$), and then have the same behaviour as the χ^x term further above the transition. This MFA behaviour is in no way similar to that found in the RPA. That is, our results are an example of the pronounced effects of short-range correlations and quantum fluctuations. The RPA scheme gives a much lower value of the Néel temperature than MFA does ($T_N \sim 0.3J$), but in a broad T region above the Néel point strong short-range correlations exist, and the RPA includes the manner in which these fluctuations strongly modify the susceptibility. Similar reasoning explains the differences in χ^x between the MFA and RPA.

For completeness, in Figs. 10,11,12 we present all components of the susceptibility together, within both the MFA and the RPA, contrasting different values of the physical parameters describing the DM interaction. To be specific, in Fig. 10 we show the situation when $\varepsilon_1 > \varepsilon_2$ with the ratio $(\varepsilon_1/\varepsilon_2)^2 \approx 4.2$ at zero temperature. As a result, we obtain that for $T = 0$ $\chi^y < \chi^x, \chi^z$ with the same ratio between the x, z and y components of susceptibility $\chi^{x,z}/\chi^y \approx 4.2$ (see §IV D). By increasing the magnitude of the DM parameter d, due to the strong dependence of the mode ε_2 of the d (see Fig. 4), we obtain the situation corresponding to $\varepsilon_2 = \varepsilon_1$. Then, as is seen in Fig. 11, both the MFA and RPA schemes result in equal values of the all components of susceptibility at low T. A further increasing of d leads to the situation $\varepsilon_2 > \varepsilon_1$, opposite to the one presented in Fig. 10. In Fig. 12 we show the susceptibility in the case of the ratio $(\varepsilon_2/\varepsilon_1)^2 \approx 2.0$, and at $T = 0$ one finds $\chi^y > \chi^x, \chi^z$ and $\chi^y/\chi^{x,z} \approx 2.0$ for $T = 0$. (We note that for other sets of $d, \Delta\Gamma$, the behaviour of the components of χ is
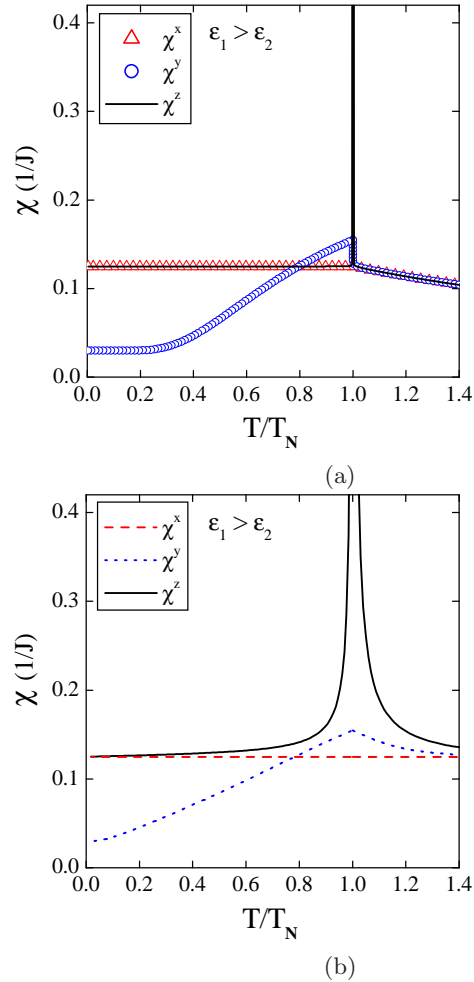

FIG. 10: (Color online) All 3 components of the susceptibility within (a) the MFA, and (b) within the RPA, for $d/J = 0.02$ and $\Delta\Gamma/J = 0.42 \times 10^{-3}$.

determined almost entirely by the ratio of the spin-wave gaps, $\varepsilon_1/\varepsilon_2 =$. These results agree with our analytical predictions (see section IV).)

Then, comparing the z-component of the susceptibility within the RPA (Figs. 10(b)-12(b)) we also find that increasing of the anisotropy parameter d leads to the broadening T regions where (i) the effects of the quantum fluctuations are important $T < T_N$ and (ii) the strong short-range correlations exists $T > T_N$.

VI. SUMMARY AND CONCLUSIONS/DISCUSSION

To summarize, we have presented a theoretical investigation of a single CuO$_2$ plane of the undoped La$_2$CuO$_4$ crystal in the low-T orthorhombic phase. The Cu spins in the plane were modelled by the 2D spin-1/2 Heisenberg AF with spin-orbit coupling, the latter represented the antisymmetric and symmetric DM anisotropies. We have adopted the Green's function
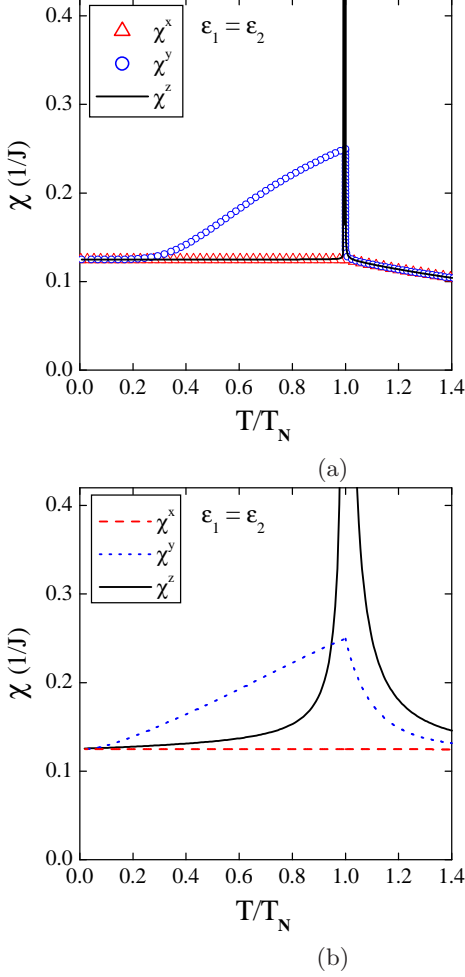
FIG. 11: (Color online) All 3 components of the susceptibility within (a) the MFA, and (b) within the RPA, for $d/J = 0.041$ and $\Delta\Gamma/J = 0.42 \times 10^{-3}$.
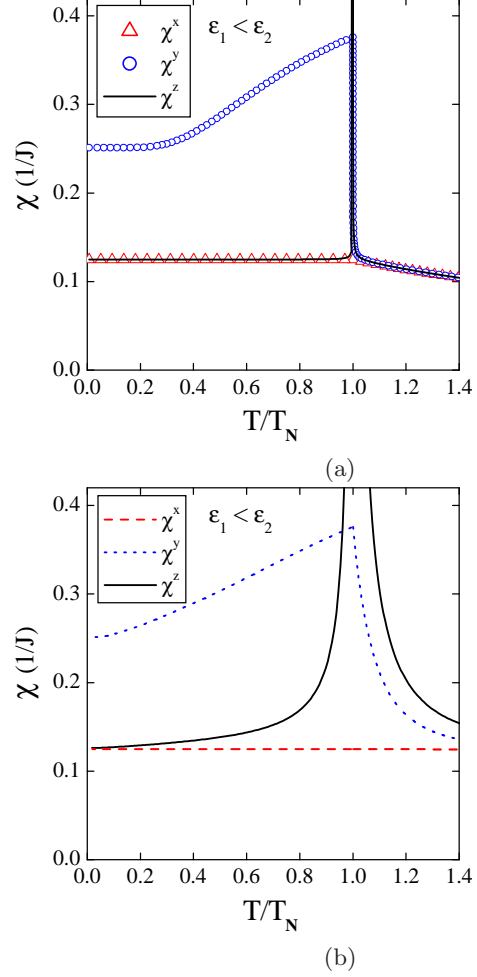

FIG. 12: (Color online) All 3 components of the susceptibility within (a) the MFA, and (b) within the RPA, for $d/J = 0.058$ and $\Delta\Gamma/J = 0.42 \times 10^{-3}$.

method within Tyablikov's RPA decoupling scheme to calculate the magnetic susceptibility of such a model. In order to allow us to accurately model the longitudinal susceptibility within such a level of decoupling of high-order Green's functions, we have extended Liu's method[17] for the isotropic Heisenberg model to one that includes a weak canted FM moment in the plane.

We can emphasize several important conclusions from our results. We have found that the anisotropy introduced into the problem by the symmetric and antisymmetric DM interactions leads to important changes in the behaviour of the magnetic susceptibility near the transition point. By comparing the MFA and RPA results we conclude that the effects of quantum fluctuations and the short-range correlations are very strong in the *broad temperature region* of near the Néel temperature. Further, we find that since the RPA and SW results are quite different near the Néel temperature, the effects of spin-wave interactions, which are included in an approximate way in the RPA but not the SW theories, are very important in this system. This neces-

sarily leads to the question, would more advanced decoupling schemes, namely improvements on Tyablikov's decoupling (*e.g.*, see our Eq. (59)), or, possibly, the inclusion of nonlinear effects in the SW theory, lead to qualitatively different results?

Secondly, we have obtained that the weak ferromagnetism in the z-direction (caused by the DM interaction) leads to the essential difference between the temperature behaviours of the transverse χ^x and χ^z components of the susceptibility (recall that the AF moments lie in the $y - z$ plane and are nearly aligned along the y axis). We established the correlation between the ratio of the in- and out-of-plane spin-wave modes of the excitation spectrum in the long wavelength limit ($\boldsymbol{k} = 0$), which is fixed by the ratio between the d and $\Gamma_1 - \Gamma_3$ DM parameters, and the behaviour of $\chi^{x,z}$ *vs.* χ^y in the zero temperature limit. This conclusion is independent on the analytical method which we used to calculate the susceptibilities, since all methods agree in the low-T regime, and could allow one to make predictions concerning the gaps in the excitation spectrum based on the data for the suscepti-

bility.

Now we comment on the comparison of our results to the experimentally observed anisotropies[6] that motivated this work. We can state that, in addition to the known results[12,13,14] that DM interaction induces the weak ferromagnetism in the LTP phase and the spin-wave gaps, this interaction is at least in part responsible for the unusual anisotropy in the magnetic susceptibility.[6] We can mention the most significant features observed in the experiment that are in qualitative agreement with the presented in paper theoretical results: (i) the absence of any special behaviour (anomaly) in the transverse component χ^x across the Néel temperature; (ii) the additional increase of the χ^y component in the ordered state and its smooth decrease in a broad temperature region in the paramagnetic state; (iii) a significant temperature dependence of the component χ^z in the broad temperature region below and above the transition point.

Now we briefly discuss the experimental data which cannot be explained within the framework of the proposed here theory. Firstly, we have found that the observed ratio between the x and y components $\chi^x < \chi^y$ (in the $T = 0$ limit) takes place only if the spin-wave gap with out-of-plane mode is less than the in-plane one $\varepsilon_o < \varepsilon_i$. However, older neutron-scattering experiments[5] find the opposite ratio: the magnitude for the out-of-plane mode is 5 meV, for the out-of-plane mode 2.3 meV. Recent Raman work confirms one of these values.[32] So, other interactions which affect these gaps must be important for an accurate explanation of the susceptibility data. Secondly, our results cannot explain a T-independent shift between χ^x, χ^y and χ^z observed in experiments – an explanation of this physics is provided in the experimental paper, namely that one must include a van Vleck contribution which shifts, in a T-independent manner, these components of the susceptibility, but we defer our inclusion of this physics until the second paper in this series of theoretical studies.

For further improvements of our theoretical modelling of the La_2CuO_4 compound, it seems to be important to investigate a 3D model on a body-centered lattice with the weak AF interlayer coupling. It is also possible to extend the 2D model by considering the ring exchange, and the interaction between the next nearest neighbour sites, and we expect that some of these additional physics can be responsible for the correct ratio between the spin-wave gaps with respect to the ratio between χ^x and χ^y. In addition, the anisotropic Van Vleck contribution (orbital susceptibility) and gyromagnetic (Landé) factor need to be taken into account. We will present a detailed comparison to these experiments when these other interactions are included in future publications.

[*] Electronic address: tkir@physics.queensu.ca

[1] A.J. Millis, H. Monien, and D. Pines. *Phys. Rev. B*, 42:167, 1990.

[2] E. Manousakis. *Rev. Mod. Phys.*, 63:1, 1991.

[3] T. Thio, T.R. Thurston, N.W. Preyer, P.J. Picone, M.A. Kastner, H.P. Jenssen, D.R Gabbe, C.Y. Chen, R.J. Birgeneau, and A. Aharony. *Phys. Rev. B*, 38:905, 1988.

[4] M.A. Kastner, R.J. Birgeneau, T.R. Thurston, P.J. Picone, H.P. Jenssen, D.R. Gabbe, M. Sato, K. Fukuda, S. Shamoto, Y. Endoh, K. Yamada, and G. Shirane. *Phys. Rev. B*, 38:6638, 1988.

[5] B. Keimer, R.J. Birgeneau, A. Cassanho, Y. Endoh, M. Greven, M.A. Kastner, and G Shirane. *Z. Phys. B*, 91:373, 1993.

[6] A.N. Lavrov, Y. Ando, S. Komiya, and I. Tsukada. *Phys. Rev. Lett.*, 87:0170071, 2001.

[7] I. Dzialoshinski. *J. Phys. Chem. Solids*, 4:241, 1958.

[8] T. Moriya. *Phys. Rev.*, 120:91, 1960.

[9] J. Stain. *Phys. Rev. B*, 53:785, 1996.

[10] In this notation the c axis points perpendicular to the cuo2 plane.

[11] T. Thio and A. Aharony. *Phys. Rev. Lett.*, 73:894, 1994.

[12] D. Coffey, T.M. Rice, and F.C. Zhang. *Phys. Rev. B*, 44:10 112, 1991.

[13] L. Shekhtman, O. Ebtin-Wohlman, and A. Aharony. *Phys. Rev. Lett.*, 71:468, 1993.

[14] W. Koshibae, Y. Ohta, and S. Maekawa. *Phys. Rev. B*, 50:3767, 1994.

[15] J. Stain, O. Ebtin-Wohlman, and A. Aharony. *Phys. Rev. B*, 53:775, 1996.

[16] S.V. Tyablikov. *Ukrain. Mat. Zh*, 11:287, 1959.

[17] K.H. Lee and S.H. Liu. *Phys. Rev.*, 159:390, 1967.

[18] D.P. Arovas and A. Auerbach. *Phys. Rev. B*, 38:316, 1988.

[19] S. Sarker, C. Jayaprakash, H.R. Krishnamurthy, and M. Ma. *Phys. Rev. B*, 40:5028, 1989.

[20] T.N. de Silva, M. Ma, and F.C. Zhang. *Phys. Rev. B*, 66:104417, 2002.

[21] M. Takahashi. *Phys. Rev. B*, 40:2494, 1989.

[22] V.Yu. Irkhin, A.A. Katanin, and M.I. Katsnelson. *Phys. Rev. B*, 60:1082, 1999.

[23] I. Affleck and J.B. Marston. *Phys. Rev. B*, 37:3774, 1988.

[24] A. Sherman and M. Schreiber. *Phys. Rev. B*, 63:214421, 2001.

[25] Yu.A. Izyumov, N.I. Chaschin, and V.Yu. Yushankhai. *Phys. Rev. B*, 65:214425, 2002.

[26] S. Chakravarty, B.I. Halperin, and D.R. Nelson. *Phys. Rev. B*, 39:2344, 1989.

[27] David C. Johnston. *Handbook of Magnetic Materials*, 1996.

[28] N.E. Bonesteel. *Phys. Rev. B*, 47:11302, 1993.

[29] D. Coffey, K.S. Bedell, and S.A. Trugman. *Phys. Rev. B*, 42:6509, 1990.

[30] D. Mermin and X. Wagner. *Phys. Rev. Lett.*, 17:1133, 1966.

[31] S.H. Liu. *Phys. Rev.*, 142:267, 1967.

[32] A. Gozar, B.S. Dennis, G. Blumberg, S. Komiya, and Y. Ando. *Phys. Rev. Lett.*, 93:027001, 2004.

[33] C.J. Peters, R.J. Birgeneau, M.A. Kastner, H. Yoshizawa, Y. Endoh, J. Tranquada, G. Shirane, Y. Hidaka, M. Oda, M. Suzuki, and T. Murakami. *Phys. Rev. B*, 37:9761, 1988.